KTH Industrial Engineering and Management

Master of Science Thesis

Department of Energy Technology

KTH 2020

Performance Evaluation of a High Temperature Borehole Thermal Energy Storage Under Influence of Groundwater Flow

TRITA-ITM-EX 2020:617

Max Hesselbrandt

Approved	Examiner	Supervisor
	Björn Palm	Alberto Lazzarotto
	Commisioner	Contact person
	Bengt Dahlgren AB	José Acuña

Abstract

Recent years have seen a growing interest in large-scale high-temperature borehole thermal energy storage (HT-BTES) as a means to store industrial waste heat and solar energy between the seasons. A profound understanding and characterization of the thermal and hydraulic processes involved in such systems is required for the optimal design as well as for environmental assessments of the storage.

In this work, the importance of groundwater flow effects on the thermal performance of HT-BTES has been studied. The current research status on groundwater flow and transport modeling techniques applied in the field of shallow geothermal energy as well as in other geosciences disciplines has been reviewed. A finite element heat conduction model of an existing HT-BTES located in dry heterogeneous soil has been developed and validated against operational and monitoring data. The heat conduction model provided a basis by which to compare the behaviour and performance of the storage under influence of groundwater flow. Numerical experiments were conducted considering both pure heat conduction as well as different scenarios accounting for groundwater flow. A performance evaluation study based on key performance indicators in terms of energy and exergy efficiencies has been carried out to quantify the impact of groundwater flow on the amount and quality of the heat being stored and exchanged. The analysis shows that the presence of groundwater flow is in general detrimental to the energy and exergy performance of the HT-BTES. The results indicate, however, that small groundwater flow rates also can have a slight positive effect on seasonal energy and exergy efficiencies as compared to case of pure conduction. Further studies are though needed where a wider range of time scales, BHE designs, operation conditions and subsurface conditions are adressed.

From the inherent uncertainties associated with subsurface flow and transport processes it follows that general guidelines on how and under what conditions groundwater flow may have impact on BTES design and performance are difficult to provide. The characteristics of these processes in porous, and particularly fractured, media are often very site-specific and scale dependent, making it a challenging task to select and use an appropriate modeling approach that can capture all relevant features of the problem. To face this challenge, various modeling approaches, typically based on deterministic and stochastic continuum or discrete fracture network concepts, have been developed within the field of subsurface flow and transport modeling. To widen the modeling framework typically employed in shallow geothermal energy applications, their applicability also in the context of BTES modeling could be explored.

Sammanfattning

Intresset för säsongslagring av industriell överskottsvärme och solenergi genom högtemperaturborrhålslager (HT-BTES) har på senare år ökat. För att möjliggöra en optimal design av dessa system, samt för att bedöma deras inverkan på omgivande miljö, krävs djupgående förståelse och karaktärisering av de kopplade termiska och hydrauliska processer som påverkar lagret.

I detta arbete har grundvattenflödets inverkan på högtemperaturlagers termiska prestanda behandlats. Nuvarande kunskapsläge inom modellering av grundvattenflödes- och transportprocesser i porösa och sprickiga medier har granskats, liksom dess användning inom geoenergi och andra geovetenskapliga områden. En värmeledningsmodell av ett befintligt HT-BTES i torr, heterogen jord har utvecklats genom finita elementmetoden och validerats mot mätdata. Värmeledningsmodellen tillämpades som referens för jämförelse med utökade modeller i vilka inverkan av grundvattenströmning beaktats genom kopplade hydro-termiska beräkningar. En utvärdering av lagrets prestanda med avseende på nyckelindikatorer i form av energi- och exergiverkningsgrad har utförts för att kvantifiera inverkan av grundvattenflödet på mängden och kvaliteten av den värme som överförs och lagras genom borrhålslagret. Resultaten visar att förekomsten av grundvattenströmningar genom lagret generellt har en negativ inverkan på dess energi- och exergiverkningsgrad. Däremot finns det i resultaten indikationer om att låga grundvattenflöden även kan bidra till en svagt positiv effekt jämfört med fallet med ren värmeledning. Vidare och mer omfattande studier bör dock utföras där längre tidsskalor samt en större uppsättning lagerdimensioner, driftscenarion, och markförhållanden beaktas.

Till följd av att det kring strömnings- och transportprocesser i mark alltid råder inneboende osäkerheter är det svårt att upprätta generella riktlinjer kring hur och under vilka omständigheter ett grundvattenflöde kan ha inverkan på ett borrhålslagers design och prestanda. Typiskt för dessa processer i porösa och i synnerhet sprickiga medier är att de är mycket platsspecifika och skalberoende, vilket medför utmaningar vid valet av ett lämpligt modellkoncept för att beskriva dem med erfoderlig precision. Detta har lett till att ett stort antal modelleringskoncept har utvecklats och prövats för detta ändamål, vilka främst baseras på antaganden om deterministiska eller stokastiska kontinuum och diskreta spricknätverk. Tillämpbarheten av dessa modellkoncept även för modellering av HT-BTES bör undersökas och utvärderas för att möjliggöra analys av borrhålslager under inverkan av komplexa strömningsförhållanden.

Acknowledgement

I would like to express my special thanks to my supervisor Alberto Lazzarotto (KTH) for constructive advice and inspiration during this work. I am deeply grateful to José Acuña (Bengt Dahlgren AB), who created the opportunity for me to conduct this thesis as well as many more exciting projects. Thank you for giving me support and encouragement to develop my ideas. I would also thank Willem Mazzotti Pallard and Mohammad Abuasbeh (KTH) for useful discussion and suggestions.

I appreciate very much the help of DHI, and especially Sten Blomgren, who provided the license for the FEFLOW software and technical support. I am grateful to Karl Woldum Tordrup and Søren Erbs Poulsen (VIA University College) who kindly helped with providing the data used in this study.

Thanks to my colleages and friends at Bengt Dahlgren AB, with whom I have shared many happy moments.

Finally, my greatest appreciation goes to my family for their unconditional and invaluable support along the way.

Table of Contents

1 Introduction

1.1 Background

Increasing concerns on climate change and energy shortage has given rise to a growing attention towards high-performance energy technologies that harness energy sources in a sustainable manner. Waste heat recovery and thermal energy storage systems have been identified as key enablers for meeting climate neutrality targets and expanding the use of renewable energy resources (Bianchi et al., 2019; Wheatcroft et al., 2020). In climate regions where large seasonal temperature variations prevail, borehole thermal energy storage (BTES) is a promising means for meeting temporal mismatches between energy availability and demand. BTES systems consist of an array of vertical closed or open loop borehole heat exchangers (BHE) inserted into the ground. In the non-heating season months, energy from solar thermal collectors, industrial waste heat or other sources is transferred to the boreholes and stored as sensible heat in the surrounding soil or rock mass. The storage can be discharged whenever the heating demand increases, thus balancing the seasonal phase difference between energy demand and supply.

Sustainable design and operation of single and multiple BHEs has been an integral aspect in research and development of BTES technology and other types of shallow geothermal systems. Both theoretical and experimental investigations have been carried out to study reliability and long-term behavior of thermally interacting BHEs (Rybach and Eugster, 2010; Rybach and Mongillo, 2006; Signorelli et al., 2005). Major efforts have involved the development of modeling techniques for predicting and analyzing the thermal processes ocurring inside the borehole and in the surrounding ground (Eskilson, 1987; Hellström, 1991; Zeng et al., 2002). Accurate prediction of both short-term and long-term BHE fluid temperatures is crucial to the design and evalutation of BHE systems. Most existing design tools (ASHRAE, 2015; BLOCON, 2017; Pahud et al., 1996) are based on semi-analytical models for solving the spatiotemporal temperature response to a thermal load on the ground with different combinations of borehole geometries and field configurations. These tools benefit from quick calculation times, which drastically shortens the iterative process of determining appropriate dimensions of the BTES system. The mathematical models used do however rely on simplifying assumptions, viz., that the heat is transferred only by pure conduction in a homogeneous and isotropic medium (Spitler and Bernier, 2016). Consequently, any effects of groundwater flow in porous media or through fractured rock are assumed to be negligible.

Several authors have questioned the validity of these assumptions. (Chiasson et al., 2000), (Sutton et al., 2003) and (Diao et al., 2004) reported that the presence of groundwater flow may have non-negligible or significant impact on the ground resistance compared to a case of pure conductive heat transfer. Given the objective of maintaining the temperature anomalies within the storage volume as large as possible at all times, any process of heat transport across the storage boundaries will contribute to heat losses from the system and can thus have detrimental effects on the performance. Since many BTES systems rely on designs and operation strategies that are intended to promote thermal stratification inside the storage, additional heat transport due to advection may also act to smooth out temperature gradients and thus cause exergy destruction. Hence, neglecting the influence of groundwater flow in the design process may result in conservative or inadequate solutions (Spitler and Bernier, 2016; Zhang et al., 2015), and BTES systems may be negatively impacted by groundwater advection (Banks, 2015; Nguyen et al., 2017).

To date there is a paucity of literature on groundwater effects on BTES system performance (Angelotti et al., 2014). Further investigation is required to provide guidance on understanding subsurface heat transport processes in BTES applications. In addition, no consistent framework has yet been established to provide a methodology for analyzing and comparing thermal performance of BTES systems that are subjected to different subsurface and operating conditions (Lazzarotto et al., 2020). Hence, further efforts need to be undertaken in planning, design, and operation of BTES systems, including development of in-situ characterization and modeling techniques, performance optimization tools and system monitoring practices and procedures. Development of accurate simulation models and detailed energy and exergy analyses of the storage could help to improve performance and bring down uncertainties surrounding decisions about investment and implementation of BTES technologies.

1.2 Aims and objectives

This study sets out evaluate the importance of groundwater advection on the on the energy and exergy thermal performance of a high-temperature BTES. The study aims to investigate the contribution of advective heat transport to the overall heat flow and temperature degradation within and across the storage medium.

The main objectives of this work are to

1. Carry out a literature review on current research status on groundwater effects on BTES systems, and methods used in different research fields and engineering applications for modeling coupled hydro-thermal subsurface processes in various hydrogeological environments.

2. Develop and implement appropriate tools for numerical modeling of series-connected borehole heat exchanger arrays, to enable simulation of thermally stratified BTES systems with variable flow-direction control.

3. Develop a numerical 3D finite element-based pure-conduction model of an existing high-temperature BTES (HT-BTES) system located above the groundwater table and perform a model validation study using monitored operational data and ground temperature measurements. The pure-conduction model serves the purpose of validating the tool described in 2) and providing a reference scenario for comparison of thermal performance in this study.

4. Develop an extended coupled hydro-thermal model based on the reference scenario model and perform numerical experiments of the HT-BTES system accounting for heat advection, by imposing hypothetical hydraulic conditions in a saturated, confined, multi-layered porous medium.

5. Collect, define, and implement appropriate performance indicators and perform an energy and exergy thermal performance analysis based on the simulations of pure-conduction and coupled hydro-thermal models of the BTES system.

2 Literature review

In this section, a review on advective heat transport and groundwater effects in BTES and shallow geothermal applications is provided. An insight is developed into current modeling techniques and design concepts and practices in BTES development. Also given is a review of concepts and techniques for modeling of groundwater flow and heat transport employed in other related fields, such as groundwater resources management, nuclear waste disposal, and deep geothermal energy exploition.

Accurate modeling and simulation of borehole heat exchangers has been a challenging task because of the vastly varying spatial and temporal scale perspectives of the heat transport processes involved. Simulating the exchange of heat between the heat carrier fluid with the surrounding ground involves solving a local heat transport problem along an extremely slender borehole, and coupling the solution to a global problem that considers thermal processes occuring in the ground due to a single or multiple interactive BHEs. The temporal scale of these processes ranges from seconds to years, making it difficult to catch all relevant features of the processes within a single simulation model. In addition, other parameters such as groundwater movements, phase change conditions and non-uniform ground temperature distribution due to surface effects, geothermal heat flow, ground heterogeneity etc. may add complexity to the heat transport problem under consideration.

During the last decades, research on BHE modeling has mainly focused on numerical, analytical, or semi-analytical approaches for analyzing local thermal processes inside the borehole and pure conduction heat transfer processes in homogeneous and isotropic ground. Early contributions include the work by Eskilson (Eskilson, 1987; Eskilson and Claesson, 1988), who introduced the concept of g-functions to model the thermal response of single or multiple interactive BHEs, and (Hellström, 1991) who developed the duct storage model (DST) for simulating thermal processes inside heat storages consisting of uniformly placed BHEs or pile heat exchangers. (Semi-) analytical BHE modeling approaches have also been widely studied and applied to approximate the BHEs as infinite line (Carslaw and Jaeger, 1959; Ingersoll et al., 1954), finite line (Cimmino et al., 2013; Lamarche and Beauchamp, 2007; Zeng et al., 2002) or cylindrical heat sources (Bernier, 2001).

While heat conduction models have been thorougly investigated and established in design tools used for both academic and commercial purposes (Zhang et al., 2018), approaches to model advection-diffusion based heat transport processes have received far less attention in research in ground source heat pump (GSHP) and BTES technologies (Banks, 2015). In recent years, however, a growing interest has developed in groundwater effects on GSHP and BTES thermal performance and related subjects. Noteworthy studies dealing with analytical modeling of coupled groundwater flow and heat transfer in porous media are (Sutton et al., 2003) and (Diao et al., 2004), who developed ground resistance models based on the moving infinite line source (MILS) solution to the advection-diffusion equation. (Molina-Giraldo et al., 2011b) further developed the MILS theory by introducing a solution to the moving finite line source (MFLS) problem to account for axial effects and constant surface temperature, and (Katsura et al., 2020) derived an approximate solution of the moving infinite cylinder source model. (Molina-Giraldo et al., 2011a) and (Chiasson and O'Connell, 2011) also considered the effect of thermal dispersion upon advective and conductive heat transport. All these models presume simplified conditions such as homogeneous and isotropic ground material properties, uniform and steady groundwater flow, and constant ground surface temperature. However, recently developed analytical models have made it possible to account also for spatial and temporal variations in ground surface temperature (Rivera et al., 2015), and non-uniform groundwater flow in vertically-layered porous media (Hu, 2017).

Numerical models based on finite volume, finite element and finite difference methods have been proposed to better represent actual surface and subsurface conditions, or for enabling investigation of the effects of other groundwater related transport phenomena on shallow geoethermal systems (e.g. unsaturated moisture migration, freezing and thawing processes etc.). Several numerical parameter studies have been carried out to investigate the effects of groundwater flow on BHE systems with different field configurations and orientations, flow velocities, material properties, heat loading conditions etc., most of them assuming uniform 3D flow under homogeneous and isotropic ground conditions (Angelotti et al., 2014; Catolico et

al., 2016; Choi et al., 2013; Dehkordi et al., 2015b; S. Emad Dehkordi and Schincariol, 2014; Nguyen et al., 2017; Yang et al., 2013). Quite a few studies have considered heterogeneous ground conditions or groundwater flow occuring along discrete pathways; (Nguyen et al., 2015) and (Gehlin and Hellström, 2003) studied thermal impacts of groundwater flow on BHEs in heterogeneous fractured domains represented as equivalent porous media. (Gehlin and Hellström, 2003) also performed simulations considering the effect of a single, discrete fracture, and a similar approach was adopted by (Dehkordi et al., 2015a) to study the effect of multiple vertical discontinuities forming a discrete, interconnected fracture system. (Diersch and Bauer, 2014) performed numerical experiments with a BTES system in stratified soil to investigate the influence of groundwater flow on the storage efficiency, and (Luo et al., 2014) performed a comparative analysis of advection effects on thermal exchange rates in BHEs inserted in homogeneous and layered heterogeneous ground, respectively.

In general, conclusions reported in the literature show an agreement that occurence of groundwater movements can be both beneficial and detrimental to GSHP and BTES thermal performance, and that this is substantially determined by the intented mode of operation of the system. For systems operating dominantly in heat extraction or injection mode, heat advection effects are considered to have positive impact because of the tendency to reduce near-borehole temperature anomalies induced during operation. In contrast, regarding systems designed for heat storage (i.e., BTES systems), moving groundwater may carry stored heat away from the storage site, thus introducing additional losses resulting in impairment of performance. This is particularly true for HT-BTES systems, which operate at fairly elevated temperatures with respect to undisturbed subsurface temperatures. Also, under specific conditions, BTES performance may be further influenced by heat losses caused by moisture migration in the vadose zone or density-driven groundwater movements (Catolico et al., 2016; Moradi et al., 2015).

In their comprehensive review on groundwater aspects in GSHP system development, (S.E. Dehkordi and Schincariol, 2014) pointed out the lack of consideration of flow and heat advection processes given in current guidelines, regulations, and design practises concerning especially closed-loop systems. Indeed, only a few cases can be found in the literature where in-situ hydrogeological conditions have been thoroughly mapped and considered in design, operation and monitoring of existing or planned closed-loop shallow geothermal systems. Of these, most are medium to large scale or pilot BTES plants, some examples being the Crailsheim BTES (Bauer et al., 2009; Mielke et al., 2014) and Paskov BTES (Grycz et al., 2014; Rapantova et al., 2016). Besides the fact that candidate sites for implementing BTES systems are likely to be selected because of suitable hydrogeological characteristics, e.g. no or moderate occurrence of groundwater or hydraulic gradients (see for example (Lanini et al., 2014; Nordell et al., 2016; Nußbicker et al., 2003)), other possible reasons that can be brought up to explain why groundwater effects have been neglected or simplified in BTES development include lack of integration between geosciences and HVAC disciplines (S.E. Dehkordi and Schincariol, 2014) and that extensive, multidisciplinary field investigation campaigns, although necessary for optimal technical design (Luo et al., 2016), may entail high costs.

A related hurdle is that inherent compositional and spatial diversity of subsurface conditions commonly causes large variations in groundwater flow characteristics in different scales and domains, which creates difficulties in providing guidelines on, for example, critical threshold flow rates for which both advective and diffusive heat transport may be of significance. Existing attempts to provide such guidelines (Angelotti et al., 2014; Banks, 2015; Molina-Giraldo et al., 2011a) are based on assumptions of uniform groundwater flow, thus neglecting possible impacts of ground heterogeneity and anisotropy. This issue has also been addressed concerning guidelines applicable for aquifer thermal energy storage (ATES) design (Sommer et al., 2013). It is worth mentioning that values of physical properties (expressed in terms of thermal diffusivity) that govern the rate of heat conduction typically vary over a range of ~1 order of magnitude in saturated ground (Andújar Márquez et al., 2016), whereas the corresponding parameter in groundwater flow analogy (hydraulic diffusivity) can take values that span over an extreme range of orders of magnitude (Pacheco, 2013). It has also been shown that these heterogeneities appear at a wide range of spatial scales, e.g. from microscopic pore scale to macroscopic aquifer scale (Le Borgne et al., 2004; Wheatcraft and Tyler, 1988). In this context, one might raise the question whether an assumption of homogeneous and isotropic ground is applicable and adequate to meet the requirements on accuracy in modeling, design, and analysis of

monitoring data in BTES applications. If not, what spatial scale and complexity level should be considered when approaching the problem, and what is the importance of the specific geological and hydrogeological characteristics of the subsurface media?

In hydrogeology, the scale-effect problem has been a topic of discussion for many years (Berkowitz, 2002; Neuman, 1990). Various studies have reported that hydraulic properties investigated in field or laboratory appear to be functions of the scale of the test or measurement (Maréchal et al., 2004; Rovey, 1994). According to (Nastev et al., 2004), this effect can be attributed to a combination of factors, including ground heterogeneity as well as the scale and spatial repartition of the measurements.

In the field of groundwater flow and subsurface transport modeling, a wide variety of modeling approaches and conceptual models has been developed and adopted to face the challenges related to scale effects, heterogeneity, and preferential flow in porous and fractured media (Bear and Cheng, 2010; Berre et al., 2018; Konikow, 2011). Considering that many problems involve investigation of large domains at e.g., aquifer or regional scale levels, continuum approaches have been widely used for this purpose. Because most subsurface flow and transport processes involve multiple phases, i.e., solids, liquids, and gases, that exchange mass, momentum and energy, describing and solving the coupled flow and transport problem at a microscopic level would require knowledge about the exact geometry of the phase interfaces and ability to measure quantities or determine model parameters within each of the phases. Instead, these complex issues can be circumvented by regarding the problem at a macroscopic level where the properties and behaviour of the different phases at the microscopic level are spatially averaged and assigned to every point of the porous medium domain, which thus can be treated as a single continuum or multiple continua representating each phase (Bear et al., 1993).

In his well-known book on groundwater hydraulics, (Bear, 1972) described the characteristics of porous media and introduced the concept of a representative elementary volume (REV) in soil hydrology. The existence of a REV is a fundamental assumption of continuum mechanics. In the averaging procedure used for transforming quantities and variables from microscopic to macroscopic scale, the REV describes the minimum volume, or range of volumes, for which the averaged quantities are independent of the size of the averaging volume. The porous medium can be inhomogeneous on scales larger than the minimum REV scale, and some systems may contain multiple REV scales. However, if a REV cannot be found within a given domain, the domain cannot be treated as a porous medium and the continuum assumption is not valid.

A continuum approach can in certain cases be justified also for the modeling of flow and transport in fractured rock, for example if the fracture system consists of a dense network of well-interconnected fractures. In continuum models, the fractures within the formation are represented implicitly without making any geometric distinction between the fractures and the rock matrix. Many fractured rock environments do not, however, possess any homogenization scale due to the lack of scale separation in the fracture network (Berre et al., 2018). In such situations, the continuum assumption is not applicable and a discrete fracture network (DFN) approach where fractures are represented explicitly may be required to accurately capture the flow and transport dynamics in the fractured rock.

Historically, typical applications of conceptual and numerical fluid flow and transport models in fractured rock have involved simulation of nuclear waste disposals (Joyce et al., 2014; Selroos et al., 2002), petroleum reservoir exploitation (Pruess, 1985), deep enhanced geothermal energy systems (Jacquey, 2017; Kalinina et al., 2012) and underground structuring (Chen, 2010; Karimzade et al., 2017). The complex nature of flow and transport in fractured media has led to the development of numerous characterization and modeling approaches, most of which are based on either one or a combination of the above-mentioned continuum or discrete fracture network concepts. In either case a deterministic or stochastic framework can be used to describe the fracture characteristics. Extensive reviews on the topic are given by (Berkowitz, 2002) and (Neuman, 2005), and more detailed information is given by (Bear et al., 1993), (Dietrich et al., 2005), (U.S. National Committee for Rock Mechanics, 1996), and (Adler, 1999).

3 Methodology

The methodology employed in this study for examining groundwater flow effects on BTES system thermal performance is introduced in this section. An approch based on numerical experiments of a HT-BTES system in porous media is followed, for which the commercial finite element code FEFLOW 7.1 (an acronym of Finite Element subsurface FLOW simulation system) was selected for coupled flow and heat transport modeling and simulations (Diersch, 2014). Finite element methods, although computationally expensive, have proven to be effective and accurate in modeling borehole heat exchanger systems (Diersch et al., 2011a; Ozudogru et al., 2015). To circumvent the need for fully discretizing the geometry of the BHEs within the finite element grid, various numerical and analytical approaches have been proposed for modeling local flow and thermal processes within the borehole (Al-Khoury et al., 2005; Al-Khoury and Bonnier, 2006; Eskilson and Claesson, 1988). The local problem can be linked to the global problem by 1D finite element representations of the BHE coupled to the 3D porous medium discretization. Based on the models provided by (Al-Khoury et al., 2005) and (Eskilson and Claesson, 1988), further extensions to support different BHE configurations (e.g. double U-pipe and coaxial pipe BHE) have been developed by (Bauer D. et al., 2011) and (Diersch et al., 2011b) and adapted to the FEFLOW simulator. Because of the combination of wide, accurate and computionally efficient BHE modeling techniques with detailed 3D analysis capabilities of coupled subsurface hydro-thermal processes, FEFLOW was deemed to be a suitable code for assessing groundwater impacts on BTES systems.

The procedure of the numerical experiments conducted in this study is summarized below and detailed in the following subsections. The methodology comprised six main stages:

1) A dataset comprising ~5 years of operational and monitoring data from an actual pilot HT-BTES plant located in Brædstrup, Denmark, was analyzed and preprocessed following the approach by (K. W. Tordrup et al., 2017), who performed an inverse modeling study of the Brædstrup BTES based on the initial two years of operation.

2) A plug-in for enabling simulation of series-connected BHEs with flow direction control was developed using the C++ programming language with the APIs available for FEFLOW. Not only is it required to consider actual operation conditions of the Brædstrup storage, but flow direction control is generally an important aspect in BTES design for maintaining horizontal temperature stratification in the storage to improve exergetic performance (Dincer and Rosen, 2007). Taking it into consideration is thus essential in BTES thermal performance assessment and analysis.

3) A 3D pure-conduction finite element model of the Brædstrup BTES was developed, for which the subsurface thermal properties inferred by (K. W. Tordrup et al., 2017) and time-aggregated operational data were taken as model inputs. The pure-conduction model served two purposes: partly for validating the plug-in tool described above, and partly for providing a validated simulation scenario in which the Darcy flux is known to be zero throughout the model. Since the storage is actually located well above the phreatic surface (K. W. Tordrup et al., 2017), no heat transport mechanisms other than conduction are likely to have significant impact on the thermal distribution close and within the storage domain, with the only possible exceptions being unsaturated moisture flow, advective infiltration in unsaturated seepage zones or local advection in small, perched aquifers. These site characteristics, in combination with extensive monitoring data comprising subsurface temperature measurements availabe, constitute a unique opportunity for characterizing the exergetic behaviour of a HT-BTES under ideal (i.e. well known) conditions.

4) The pure-conduction finite element model was extended to include heat advection by defining a hypothetical confined groundwater system within the model domain. This was accomplished by specifying steady Dirichlet boundary conditions on opposite (upstream-downstream) borders of the domain, thus imposing a uniform hydraulic gradient across the storage site. Also, hydraulic properties based on typical values taken from literature (Heath, 1983) were attributed to the model to represent the multi-layered soil composed of unconsolidated sediments present at the Brædstrup storage site.

5) Steady-flow, transient-transport simulations of the coupled hydro-thermal model were performed with varying hydraulic gradient. The BHE boundary conditions (fixed inlet temperature and flow rate) imposed

in the simulation of the pure-conduction model were applied also in these simulations, hence the unknown time-dependent parameters describing the outlet temperature of the heat carrier fluid and the temperature field throughout the domain were obtained as a function of hydraulic gradient.

6) Suitable simulation results for evaluating energy and exergy performances of the HT-BTES were gathered from all of the simulation runs, including the simulation of the pure-conduction model as a contrasting reference to the cases affected by heat advection. Following an approach similar to the one suggested by (Lazzarotto et al., 2020), energy and exergy efficiencies evaluated both at a system level (with respect to inlet and outlet energy/exergy flows) as well as within the storage were selected as Key Performance Indicators (KPIs).

3.1 Description of the Brædstrup pilot BTES plant

The Brædstrup pilot HT-BTES was implemented in 2011-2012 as part of a local district heating facility comprising combined heat and power gas turbines, electrical and gas boilers, solar thermal collectors, and hot water storage tanks. During summer, excess heat produced by the solar thermal collectors is transferred to and stored in the BTES. The BTES is discharged during non-productive times by means of a heat pump coupled to the storage.

A detailed description of the Brædstrup BTES and the subsurface geological and thermal settings at the storage site is given by (K. W. Tordrup et al., 2017) and (Sørensen et al., 2013). In Figure 1 an overview of the system is shown, including information on the lithology of the unconsolidated Quaternary glacial deposits in the area, configurations and dimensions of BHEs and observation wells, as well as the bore field arrangement.

The storage system consists of 48 grouted double U-pipe BHEs inserted to a depth of 45 m beneath two top layers of covering soil material and mussel shell insulation, each with a thickness of 0.5 m. As indicated in Figure 1, the soils at the site consist of alternating strata dominated by clay till, silt, sand and gravel. Measured water content levels (2-8% in the sand deposits) indicate that the soil is relatively dry. During drilling of the boreholes, water seepage was however encountered in the upper clay till layer (-3 to –9 m) and at a depth slightly beneath borehole bottom (-49 m), but these findings were probably due to temporary occurrence of snowmelt water or perched water (Sørensen et al., 2013). Instead, water levels monitored in some neighboring wells indicate that the groundwater table in the area is located at a depth of around 65-70 m ("GEUS," n.d.; K. W. Tordrup et al., 2017). That is, the borehole bottoms are located well above the groundwater table and hence dry-unsaturated conditions are likely to prevail in most points within the storage.

The heat exchanger boreholes are drilled 3 m apart in a hexagonal grid system. Since two single U-pipes are insert in each borehole, the system contains a total of 96 borehole loops that can be arbitrarily interconnected in series or parallel with a great variety of possible configurations. In this case, the U-pipes are arranged in 16 different arrays. As seen in Figure 1, the BHE arrays can be grouped into two different configurations, so that each contains one U-pipe per borehole. Hence, the two U-pipes installed within the same borehole are connected to separate arrays, each of which containing six series-connected loops ordered from the center to the periphery of the storage. When the storage is operated in charging mode, the heat carrier fluid flow is directed from the center, and in the opposite direction under discharging operation. These specific array arrangements combined with the flow-switching operation strategy serve the purpose of creating horizontal thermal stratification within the storage to improve temperature retention during the storing cycle.

In addition to the heat exchanger boreholes, five observation wells have been installed at different locations within (T1, T2, T3, T5) and outside (T4) the storage as shown in Figure 1. In each of the observation wells, temperature sensors for measuring soil temperature variations have been inserted at 20 fixed depth levels ranging from 0 m to -59 m beneath the insulation layer.

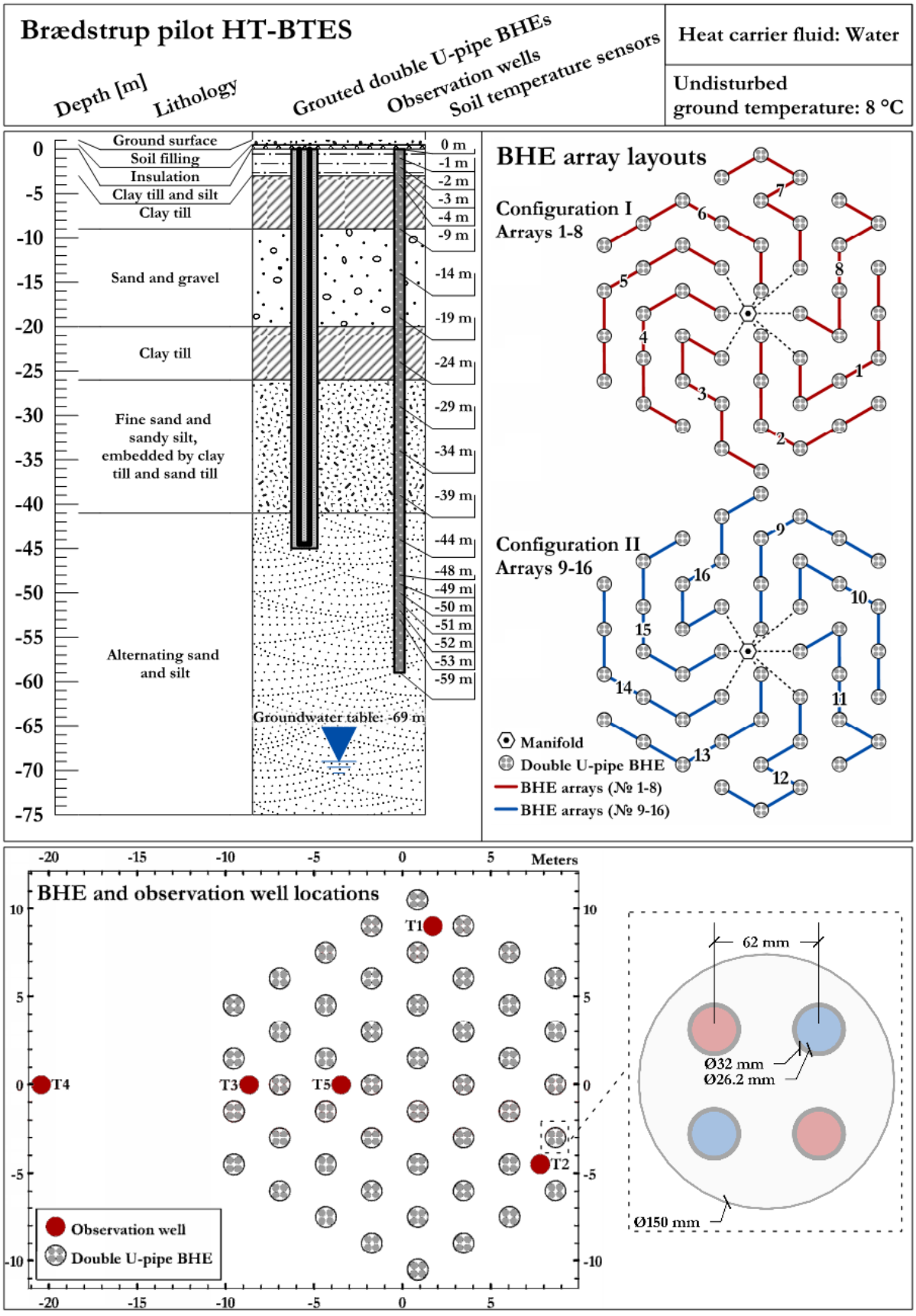

Figure 1. Overview of the Brædstrup BTES design.

3.2 Pre-processing of operational and monitoring data

The Brædstrup district heating facility has been studied on a system level by (Karl Woldum Tordrup et al., 2017), who developed a TRNSYS model of the system. Inverse modelling applied to one year of operational data was used to infer key parameters of each of the individual system components. (Tordrup et al., 2016) and (K. W. Tordrup et al., 2017) also performed detailed component level analyses of the BTES, with the objective of determining thermal properties of the heterogeneous soil strata at the storage site. A finite element model of the BTES was developed, and heat capacities and thermal conductivities were inferred by calibrating the model using operational data and distributed subsurface temperature measurements collected during the first 310 days of operation. Simulations during the following 200 days of operation (510 days in total) showed good agreement with observations of subsurface temperatures and heat extraction and injection rates.

In the present study, a larger dataset comprising 1683 days (2012-05-22 to 2016-12-31) of operational (flow rate and temperatures at BTES inlet and outlet) and subsurface temperature monitoring data has been utilized. The operational and monitoring data was used for 1) defining transient BHE BCs used as input to finite element simulation models, i.e. flow rate, inlet temperature and operation mode, as described in section 3.4, and for 2) comparisons of simulated and observed soil temperatures and return temperatures. The objective of the pre-processing procedure was to 1) identify and eliminate erroneous data, and fill in missing data, and 2) time-aggregate high-resolution data to lower resolution data, mainly for reducing the computational effort needed when performing simulations with transient BCs that swiftly vary with time.

The pre-processing procudure essentially follows the approach given in (K. W. Tordrup et al., 2017) to obtain low resolution aggregated values of soil temperatures, BTES forward/return temperatures and volumetric flow rate, with some exceptions. First, the heat carrier fluid temperature data used are the temperatures of the mixed flow at the BTES inlet and outlet, in contrast to (K. W. Tordrup et al., 2017) who considered the inlet/outlet of each individual BHE array for deriving aggregated flow rate and temperature time series. This is because a large portion of the BHE array temperature records was missing in the larger data set. Also, the data was aggregated from 5-min to 72-h resolution in the present study, as compared to 1-h to 24-h resolution in the previous study.

Before time-averaging, the high-resolution data was inspected to identify possible outliers and erroneous measurement points. For filtering the data containing forward temperature, return temperature and flow rate measurements, outlier thresholds were manually selected based on visualizations of time-ordered data as well as empirical cumulative distribution functions calculated for each vector of measurement points. The selected intervals were [0 °C, 85 °C] (forward temperature), [0 °C, 70 °C] (return temperature) and (0 m^3/h, 30.5 m^3/h] (flow rate). Data points outside these intervals as well as missing data points were replaced by interpolated values.

An energy conservation equation was set up to determine flow rate values in the low-resolution domain, according to Eq. 1 (K. W. Tordrup et al., 2017):

$$\dot{V}_l = \frac{1}{(T_{f,l} - T_{r,l})\Delta t} \int_{t}^{t+\Delta t} \dot{V}_h (T_{f,h} - T_{r,h})\, dt \tag{1}$$

where $\dot{V}_l$ is the volumetric flow rate, $T_{f,l}$ is the forward temperature and $T_{r,l}$ is the return temperature aggregated over a timestep Δt with length 72 h, and $\dot{V}_h$, $T_{f,h}$ and $T_{r,h}$ are the corresponding parameters in the high-resolution domain. Aggregated values of flow rate resulting in <0.1 m^3/h were set to zero, because the numerical solver occasionally exhibits unstable behavior when very low heat carrier flow rates are imposed. The aggregated time series of forward temperature, return temperature and flow rate are shown in Figure 2. Also shown in the figure is the net amount of energy injected into the ground calculated from the flow rate and the inlet-outlet temperature difference, assuming a volumetric heat capacity of the heat carrier fluid equal to 4.19 $MJ/m^{-3}/K^{-1}$.

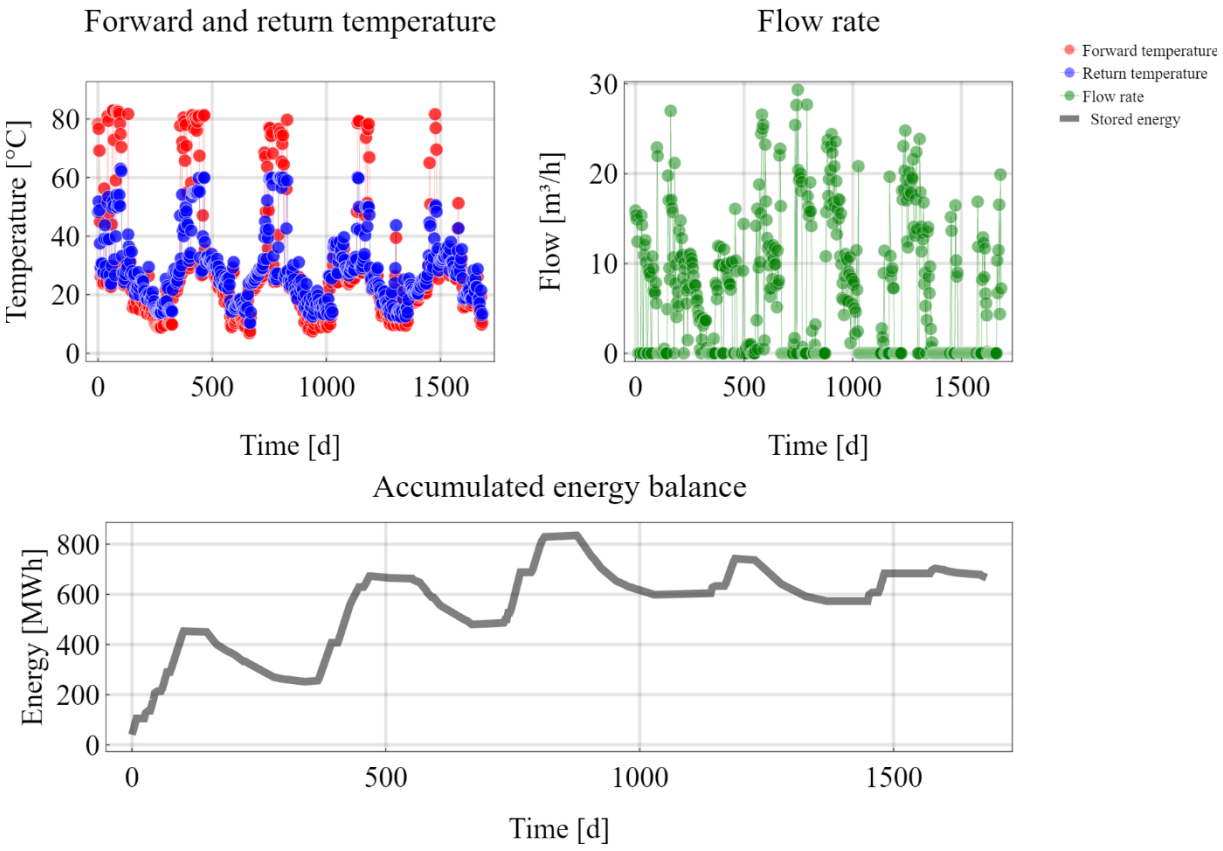

Figure 2. Top: Aggregated time series (72-h resolution) of total flow rate and BTES inlet and outlet temperatures. Bottom: Accumulated energy balance during the first 1683 days of operation.

Soil temperature records from observation wells T1-T5 were inspected visually and aggregated to 24-h resolution. Among a total of 100 time series records, 13 were omitted either because of the measurement data being erroneous or the temperature probes being located close to or on the boundary of the domain of interest (T1 at 0 m; T2 at 0 m, 34 m, 48 m; T3 at 0 m; T4 at depths 0 m, 1 m, 2 m, 3 m, 4 m, 34 m, T5 at 0 m, 44 m). The selection procedure is not further elaborated here since the soil temperature measurements were only used for visual comparison with computed soil temperatures at corresponding model points.

3.3 Plugin development for BTES system operation control

The concept of designing BTES systems using arrays of series-connected BHEs with flow-reversal capability has been adopted in several HT-BTES implementations, in addition to the Brædstrup storage (Catolico et al., 2016; Nordell, 1994; Rapantova et al., 2016). Although FEFLOW provides a built-in tool for modeling interconnected BHEs, it is not capable of modeling BHE arrays with reverse-flow operation (as of version 7.3). A plugin has therefore been developed to allow for simulations of actual operation conditions of the Brædstrup BTES and other systems with similar design and operation strategy. The plugin was developed using C++ with the FEFLOW APIs, which enable reading or modification of model parameters during simulation run-time.

Using the plugin, an arbitrary number of parallel arrays of series-connected BHEs can be defined by grouping and sorting the BHEs on the basis of an array ID and an ascending number that specifies the linking order of a borehole within an array. The lowest-order BHE within the array (e.g., № 11 in Figure 3) constitutes the array inlet during charging, and vice versa during the discharging period.

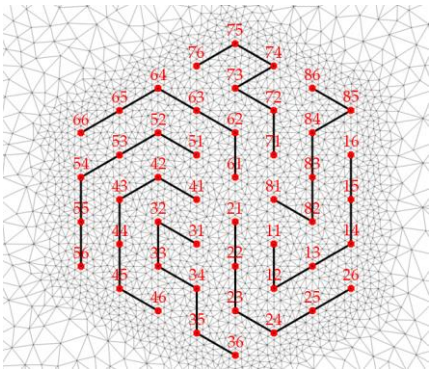

Figure 3. ID convention for defining BHE arrays and their connectivity.

The plugin controls the BHE array operation by taking three time-series as user input: 1) mode of operation (charging/inactive/discharging), 2) total flow rate and 3) inlet temperature to the storage. Before each time step or iteration, the flow rate and inlet temperature at current time are set as boundary conditions at the inlet of the first BHE of the array, according to the mode of operation. The flow is assumed to be uniformly distributed between the BHE arrays.

Since the inlet temperature at the remaining BHE inlets are unknown (and the matrix equation system representing the processes within the BHEs being inaccessible through the API), the resulting BHE outlet temperatures obtained in the previous time step or iteration are set as inflow temperature for the next BHE in the array at next time step. The number of iterations per time step may be restricted to reduce simulation time. One should though keep in mind that errors may be introduced in case rapid changes in boundary conditions or primary variable (temperature) occur, and if the time-step sizes are not sufficiently small. However, as will be shown in section 4.1, the thermal behaviour of the BHE array can be approximated quite accurately (in long-term analysis) by using automatic time-stepping control in combination with low-resolution BHE inlet boundary conditions during simulation. Further development is required for enabling analysis of short-term effects to accurately reproduce the full dynamics of series-connected BHEs.

Future improvement of the plugin will enable specifying individual boundary conditions for specific BHE arrays, as well as defining other BC options than the inlet temperature type (e.g., power and temperature difference), which would allow for detailed studies on optimization of BTES operation strategies and BHE array design. The source code will be published on https://github.com/MaxHesselbrandt/BTESrevFlow.

3.4 Pure-conduction finite element model development

To investigate thermal performance of a HT-BTES unaffected by groundwater flow, a pure-heat conduction model of the Brædstrup BTES has been developed and simulated using actual operational data (see section 3.2) as input. In combination with extensive measurement data available, the subsurface characteristics at the storage site appear to constitute favorable conditions for purposes of validation and performance analyses. Due to the storage being situated in the vadose zone well above the regional groundwater table, there is less probability that other transport mechanisms than conduction may significantly contribute to the subsurface temperature distribution observed during operation. Hence, less uncertainties exist in subsurface characterization when attempting to reproduce the thermal behaviour of the storage by means of simulation models. If a pure-conduction model proves to sufficiently estimate the observed data, the effect of groundwater flow on the subsurface thermal regime may be readily quantified by direct comparisons between the conduction model and hypothetical advective-transport models. The latter would also give an insight on how the real system would have performed under the influence of groundwater flow.

Another objective of the pure-conduction model was to validate that the FEFLOW plugin tool described in section 3.3 is capable of capturing the long-term behaviour of BHE arrays in an accurate manner. Besides being important for predicting heat exchange rates for the BTES system, an accurate representation of the temperature distribution close to the boreholes is crucial for understanding groundwater effects on storage stratification and factors affecting exergy destruction within the storage.

At the Brædstrup storage site dry-unsaturated conditions prevail, meaning that transient heat transport in the soil is either handled by the 3D heat conduction equation (Carslaw and Jaeger, 1959) or by differential equations describing coupled unsaturated flow and heat transport phenomena, e.g. (DHI-WASY, 2009). It is assumed here that heat transport occurs only by thermal conduction. However, for convenience, throughout this study the model domain is treated as a confined, saturated porous medium with bulk thermal properties equivalent to that of a dry medium. This way, the pure-conduction model can be extended to also account for heat advection only by imposing non-zero hydraulic boundary conditions onto the model domain. This means that the medium is assumed to have porosities saturated by groundwater, described by the volume fraction ε. The conservation equation of thermal energy in a saturated porous medium g, consisting of a solid phase s and a fluid phase f, reads as (Diersch et al., 2011b)

$$\frac{\partial}{\partial t}\left\{\left[\varepsilon\rho^f c^f + (1-\varepsilon)\rho^s c^s\right]T_g\right\} + \nabla\cdot\left(\rho^f c^f \boldsymbol{q} T_g\right) - \nabla\cdot\left(\boldsymbol{\Lambda}\cdot\nabla T_g\right) = Q, \tag{2}$$

where $\boldsymbol{q}$ is the flux expressed by Darcy's law, ρ and c are the density and specific heat capacity of the phases (indicated by their respective superscript), T_g is the temperature of the saturated medium, Q is a heat sink/source term (e.g., due to a BHE), and $\boldsymbol{\Lambda}$ is the tensor of thermal hydrodynamic dispersion written as

$$\boldsymbol{\Lambda} = \left[\varepsilon\lambda^f + (1-\varepsilon)\lambda^s\right]\boldsymbol{I} + \rho^f c^f\left[\alpha_T\|\boldsymbol{q}\|\right]\boldsymbol{I} + (\alpha_L - \alpha_T)\frac{\boldsymbol{q}\otimes\boldsymbol{q}}{\|\boldsymbol{q}\|}. \tag{3}$$

In Eq. 3, α_L and α_T are the longitudinal and transverse thermodispersivities, respectively, λ is the thermal conductivity, and $\boldsymbol{I}$ is the identity matrix. In the case of pure conduction, $\boldsymbol{q}$ is a zero vector, thus Eq. 2 reduces to the heat conduction equation

$$(\rho c)_g\frac{\partial T_g}{\partial t} - \nabla\cdot(\boldsymbol{\lambda}\cdot\nabla T_g) = Q, \tag{4}$$

where $(\rho c)_g = \varepsilon\rho^f c^f + (1-\varepsilon)\rho^s c^s$ is the bulk volumetric heat capacity and $\boldsymbol{\lambda} = \lambda_g\boldsymbol{I} = \left[\varepsilon\lambda^f + (1-\varepsilon)\lambda^s\right]\boldsymbol{I}$ is the bulk thermal conductivity of the porous medium.

For solving the heat conduction problem, the finite element method has been applied using FEFLOW 7.1 for mesh construction, modeling, and simulation. The model domain consists of a rectangular prism with dimension of 600 m × 200 m × 80 m. Even though a rather uniform temperature field is expected to evolve around the BHEs in the case of conductive heat transfer, the domain is elongated along the x-axis to capture downstream temperature dynamics in simulations of the extended model where groundwater flow is assumed (see section 3.5). The domain was discretized by first constructing a 2D unstructured mesh using a triangulation code which is capable of generating exact Delaunay triangulations (Shewchuk, 1996). The 3D mesh structure was set up by extruding the 2D mesh along the depth direction (z-axis) to create a vertically structured grid partitioned into 61 plane layers of triangular prismatic elements, with thicknesses of 1 m for layers in the depth interval 0-59 m and between 1 m to 4.2 m at larger depths. The discretization procedure resulted in a 3D mesh consisting of 1 018 029 elements.

In FEFLOW, BHEs are modeled as 1D representations of the real geometry of the piping material and borehole filling (see for details (DHI-WASY, 2010; Diersch et al., 2011b) by imposing BHE BCs on nodes linked along vertical edges of the discretization. The horizontal 2D mesh was locally refined in the interspace region between the BHE nodes, as well as the area surrounding the BTES with emphasis on the downstream region where the thermal front migrates in the presence of groundwater movements. Specifically, the mesh around the BHEs is designed in such that an ideal spacing between the BHE nodes and respective surrounding nodes is applied to attain highest numerical accuracy, for reasons elaborated by (Diersch et al., 2011a). The mesh in the surrounding of the BHE nodes is shown in an overview of the model discretization in Figure 4, where the positions of the BHE representations are also indicated (linked in accordance with Configuration I shown in Figure 1).

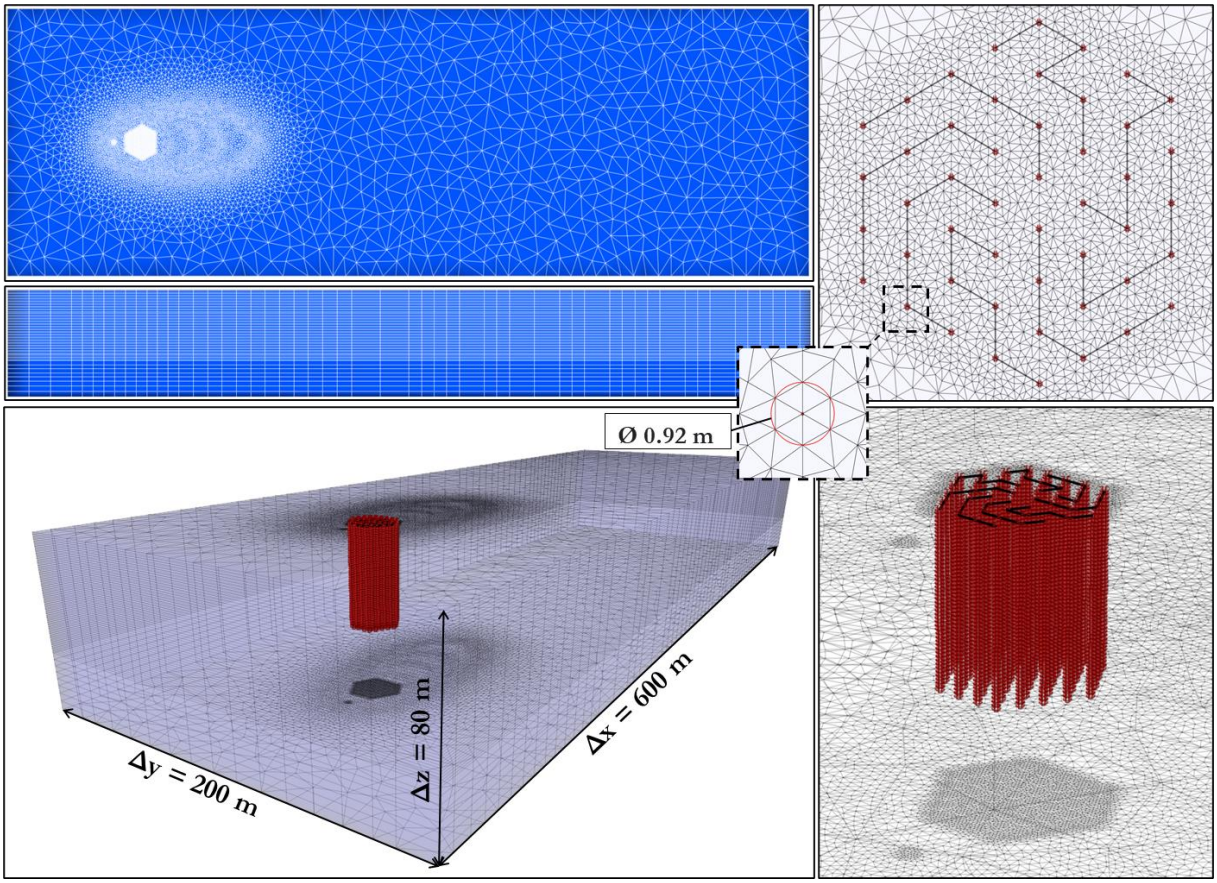

Figure 4. Overview of the model discretization.

The BHE BCs extend from the top of the model (z = 0 m) down to a depth of 45 m. The layers of heat insulation and soil fill located above the BTES at the actual site are not included in the model. Instead, the top boundary as well as the lateral and bottom boundaries are assumed to be adiabatic and thus no thermal interaction with the ground surface is accounted for. Consequently, all heat flow across the model boundaries occurs through the BHEs. Based on soil temperature measurements recorded before operation of the Brædstrup storage was initiated, an initial condition T_0 of 8 °C was set throughout the model domain.

Model parameters describing the bulk thermal properties of the vertically-layered porous media are obtained from (K. W. Tordrup et al., 2017). In their study, estimates of bulk thermal conductivity and volumetric heat capacity values for six different geological layers were inferred by inverse modeling of observed operational and soil temperature data. They found that the energy balance prediction ability of the model was improved when accounting for soil heterogeneity, in comparison with simulations of a model assuming homogeneous soil properties based on the the results of a standard thermal response test performed at the Brædstrup storage site. Since the double U-pipes in each BHE cannot be handled separately in FEFLOW, each of the two BHE array configurations of the storage (shown in Figure 1) cannot be represented correctly within the same model. Therefore, (K. W. Tordrup et al., 2017) carried out two parameter analyses for each of the configurations, assuming that both U-pipes within each borehole were identically linked to the U-pipes in previous and next BHEs in the array. The final parameter estimates were taken as the average of the estimates obtained from respective analysis.

In the present study only Configuration I has been considered, and the corresponding bulk material parameter estimates presented by (K. W. Tordrup et al., 2017) were adopted in the model, see Table 1. A porosity of 0.2 m^3/m^3 was assumed for all layers, and the material properties for each phase were accordingly adjusted and assigned to the model so that input parameters equivalent to the bulk property values were set (see Eq. 2 and Eq. 3). For the numerical solution of the heat conduction problem, isotropic conditions are assumed.

Table 1. Material properties of the vertically layered subdomains within the model.

Formation	Extent from top boundary [m]	Porosity [m³/m³]	Thermal conductivity [W/m/K]			Volumetric heat capacity [MJ/m³/K]		
		ε	λ^f	λ^s	$\boldsymbol{\lambda_g}$[1]	$\rho^f c^f$	$\rho^s c^s$	$(\boldsymbol{\rho c})_g$[1]
Clay till and silt	0-3	0.2	0.6	2.68	**2.26**	4.18	1.51	**2.04**
Clay till	3-9	0.2	0.6	1.61	**1.41**	4.18	1.79	**2.27**
Sand and gravel	9-20	0.2	0.6	1.84	**1.59**	4.18	1.06	**1.68**
Clay till	20-26	0.2	0.6	1.70	**1.48**	4.18	1.68	**2.18**
Fine sand and sandy silt, embedded by clay till and sand till	26-41	0.2	0.6	2.05	**1.76**	4.18	1.39	**1.95**
Alternating sand and silt	41-80	0.2	0.6	2.86	**2.41**	4.18	1.24	**1.83**

[1] (K. W. Tordrup et al., 2017)

The BHE heat transfer problem was considered using the parameters and settings listed in Table 2. Further information on the geometric relations of the double U-pipe BHEs is given in subsection 3.1.

Table 2. Details on parameter settings used for local BHE problem.

Parameter	Value	Unit
№ of BHEs	48	[-]
№ of BHE arrays	8	[-]
BHE array configuration	I*	[-]
BHE length	45	[m]
BHE diameter	0.15	[m]
Volumetric flow rate	Transient**	[m³]
Inlet temperature BC	Transient**	[°C]
Flow direction of heat carrier fluid	Transient**	[-]
Pipe configuration	2U	-
Shank spacing	0.062	[m]
U-pipe outer diameter	0.032	[m]
U-pipe wall thickness	0.0029	[m]
U-pipe thermal conductivity	0.42	[W/m/K]
Grout thermal conductivity	1.44	[W/m/K]
Heat carrier fluid	Water	[-]
Volumetric heat capacity of heat carrier fluid	4.19	[MJ/m³/K]
Thermal conductivity of heat carrier fluid	0.614	[W/m/K]
Dynamic viscosity of heat carrier fluid	7.97e-4	[kg/m/s]
Density of heat carrier fluid	996	[kg/m³]
BHE thermal resistance	Calculated***	[-]
Computational method	Quasi-stationary analytical (Eskilson-Claesson)****	[-]

* See section 3.1/Figure 1.

** See section 3.2 and 3.3.

*** (DHI-WASY, 2010)

**** (Eskilson and Claesson, 1988)

The simulation parameters used are shown in Table 3. A simulation of 1683 days was performed, equal to the duration of the observed data series available after operation start (see subsection 3.2).

Table 3. Parameters and conditions used for the simulation.

Parameter	Value	Unit
Simulation time period	1683	[d]
Time step control	Automatic	[-]
Initial time step length	1e-6	[d]
Predictor-corrector scheme	Forward Adams-Bashforth / Backward Trapezoid	[-]
Maximum iterations per time step	1	[-]
Error tolerance (Euclidian L^2 norm)	1e-4	[-]

3.5 Coupled hydro-thermal modeling

The pure conduction model described in section 3.4 was extended to investigate the influence of groundwater flow on the performance of the BTES. For this purpose, a hypothetical groundwater system has been considered assuming steady-flow, transient-transport in a confined, saturated porous medium. Based on the vadose zone lithological profile at the Brædstrup storage site, hydraulic properties and thermodispersivity were attributed to the model layers using typical values from literature. As can be seen in Figure 5, first-type boundary conditions were fixed on upstream and downstream lateral boundaries to impose a uniform hydraulic gradient across the domain, whilst impermeable boundaries were imposed on the remaining boundaries. The solution of the problem is a steady heterogeneous flow field that can be coupled to the heat transport problem according to Eq. 2 in subsection 3.4.

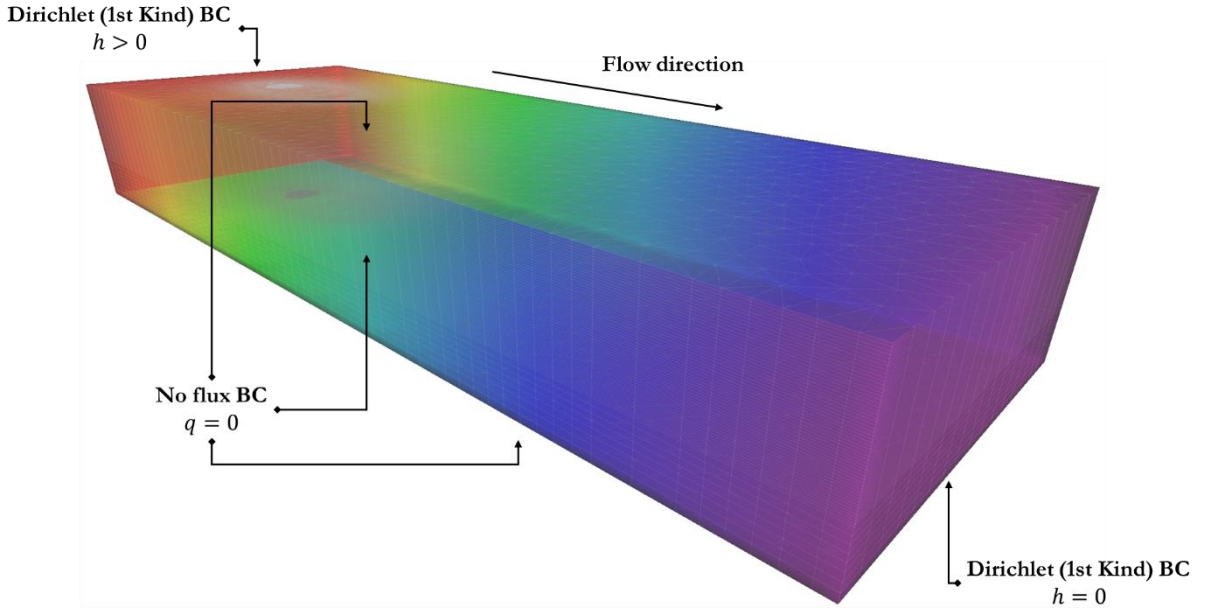

Figure 5. Hydraulic boundary conditions applied to the coupled hydro-thermal model.

Soil characterization performed at the storage site showed the presence of layered sequences of primarily clay till, silt, sand, and gravel (Sørensen et al., 2013). Under saturated conditions, the hydraulic characteristics of these soil types may vary greatly depending on composition and geometrical properties. Fine-grained clayey materials have typically high porosity but low permeability, whereas the intergranular pore spaces in coarser-grained sand and gravel materials permit water to flow relatively freely thus contributing to higher permeability. To the geological layers considered in the pure-conduction model, hydraulic conductivities (assuming isotropic conditions) were attributed based on typical values found in the literature, e.g. (Heath,

1983; Lakshmanan, 2011). As shown in Figure 6, the groundwater flow model consists of three zones with relatively high hydraulic conductivity and three low-transmissivity zones representing the sandy and clayey layers, respectively. Dispersivity of the soil were assumed to be 5 m in the longitudinal direction and 0.5 m in the transverse direction for all layers.

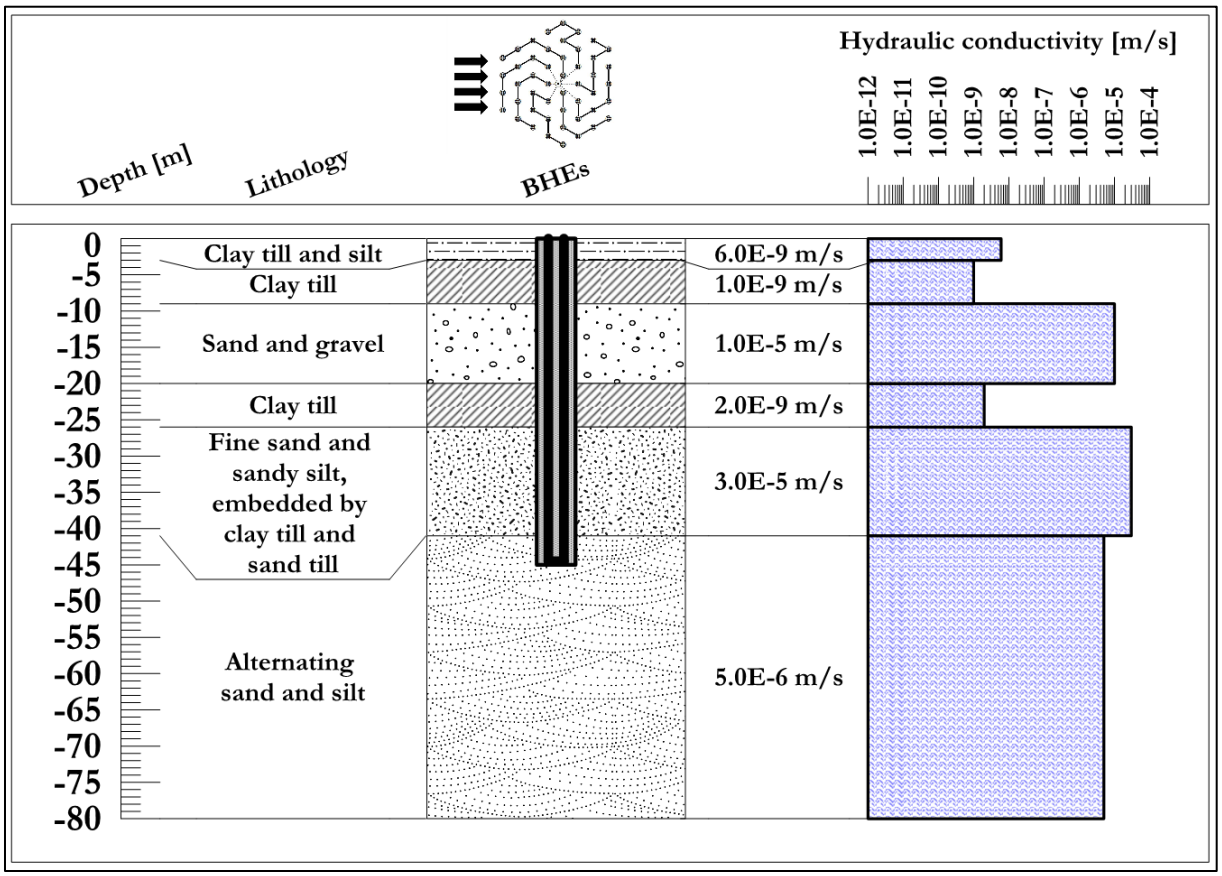

Figure 6. Hydraulic properties of the layered soil.

With a fixed hydraulic head of 0 m set on the downstream boundary nodes, five rounds of simulations were performed (including the pure-conduction base scenario) where the hydraulic head set on the upstream boundary nodes was altered to observe the effect of different hydraulic gradients across the model domain, see Table 4. For each of the simulations, all other material properties, boundary conditions and simulation parameters were maintained equal to those used in the simulation of the pure-conduction scenario described in section 3.4.

Table 4. Summary of scenarios for model simulation.

Scenario №	Upstream hydraulic head BC [m]	Downstream hydraulic head BC [m]	Hydraulic gradient [%]
1	0	0	0
2	1	0	-0.17
3	5	0	-0.83
4	7	0	-1.17
5	10	0	-1.67

3.6 Energy and exergy performance evaluation

In literature, BTES system performance is commonly assessed and quantified with respect to a ratio representing the amount of thermal energy injected to versus extracted from the BTES during a storing cycle, e.g., (Bauer et al., 2009; Nilsson, 2020; Nußbicker et al., 2003). Common names are storage efficiency,

energy efficiency or utilization ratio. As pointed out by (Dincer and Rosen, 2007), assessing the storage performance only by energy analysis has some shortages associated with loss of information on availability and quality of the heat being stored and discharged. They emphasized the importance of exergy analysis as a complement to energy analysis for assessing, comparing, and improving thermal energy storage performance. Exergy analysis has been applied in a few studies of BTES and GSHP systems (Hepbasli, 2005; Kizilkan and Dincer, 2012; Ozgener et al., 2005; Sharqawy et al., 2009), but has not been established as a standard method in shallow geothermal system design.

In this study, an approach based on the work by (Lazzarotto et al., 2020) has been implemented for assessment of BTES system energy and exergy performance. In their paper, relevant parameters for energy analysis as well as exergy and temperature analysis were formulated and evaluated at storage boundaries, i.e., at inlet and outlet but also with respect to a subsurface interface between the storage volume and surrounding ground. A 2D analytical BHE model based on the infinite line source was utilized to demonstrate their approach.

Performance indicators for quantifying system as well as storage energy and exergy efficiencies used by (Lazzarotto et al., 2020) are defined as follows:

Seasonal system performance indicators

$$\eta_{Q,system} = \frac{Q_d}{Q_c} = \frac{\int_{\tau_c}^{\tau_c+\tau_d} \dot{m}(t) c_p \left[T_r(t) - T_f(t)\right] dt}{\int_0^{\tau_c} \dot{m}(t) c_p \left[T_f(t) - T_r(t)\right] dt} \quad (5)$$

$$\psi_{Ex,system} = \frac{Ex_d}{Ex_c} = \frac{\int_{\tau_c}^{\tau_c+\tau_d} \dot{m}(t) c_p \left\{\left[T_r(t) - T_f(t)\right] - T_0 \ln \frac{T_r(t)}{T_f(t)}\right\} dt}{\int_0^{\tau_c} \dot{m}(t) c_p \left\{\left[T_f(t) - T_r(t)\right] - T_0 \ln \frac{T_f(t)}{T_r(t)}\right\} dt} \quad (6)$$

Storage performance indicators

$$\eta_{Q,storage}(\Omega, t) = \frac{Q_{stored}(\Omega, t)}{Q_{exchanged}(t)} = \frac{\int_\Omega \left(\rho(\boldsymbol{x}) c_p(\boldsymbol{x})\right)_g \left[T(\boldsymbol{x}, t) - T_0(t)\right] d\Omega}{\int_0^t \dot{m} c_p \left[T_f(t) - T_r(t)\right] dt} \quad (7)$$

$$\psi_{Ex,storage}(\Omega, t) = \frac{Ex_{stored}(\Omega, t)}{Ex_{exchanged}(t)} = \frac{\int_\Omega \left(\rho(\boldsymbol{x}) c_p(\boldsymbol{x})\right)_g \left\{\left[T(\boldsymbol{x}, t) - T_0(t)\right] - T_0 \ln \frac{T(\boldsymbol{x}, t)}{T_0}\right\} d\Omega}{\int_0^t \dot{m}(t) c_p \left\{\left[T_f(t) - T_r(t)\right] - T_0 \ln \frac{T_f(t)}{T_r(t)}\right\} dt} \quad (8)$$

Description of parameters in Eq. 5 to Eq. 8 is given below. It should be noted that the unit for temperature in Eq. 6 and Eq. 8 is Kelvin.

Q	Thermal energy	Ex	Thermal exergy	c_p	Heat carrier specific heat capacity	Subscripts			
τ	Time duration	$\dot{m}$	Heat carrier mass flow rate	Ω	Storage domain/volume	c	Charging	d	Discharging
T	Temperature	$(\rho c_p)_g$	Ground volumetric heat capacity			f	Forward	r	Return
$\boldsymbol{x}$	Spatial coordinate	T_0	Reference temperature						

As can be understood from Eq. 5-Eq. 8, theory and methods of energy and exergy analyses are similar, with a few differences. In Eq. 6 and Eq. 8, the temperature of the heat exchange as well as the quality of the heat being stored is reflected by the introduction of a reference temperature T_0, as is further described by (Dincer and Rosen, 2007) in their elaborate review on exergy storage. In this study, the undisturbed ground temperature of 8 °C (281.15 K) was chosen as reference temperature for evaluation of the exergy performance indicators.

By introducing the volume of the storage domain Ω in Eq. 7 and Eq. 8, it is possible to reflect the amount of heat and exergy being lost (or destroyed, from an exergy perspective) to the ambient ground in relation to the amount being stored and recovered. However, a BTES has intuitively no bottom or lateral boundaries, hence the storage domain is indefinite. (Lazzarotto et al., 2020) get around this issue by defining the storage domain as a volume (or area in 2D problems) containing a certain portion $(1-\epsilon)$ of the total amount of energy in the ground after a characteristic time τ of heat injection:

$$Q_{stored,\epsilon,\tau}(\Omega_{\epsilon,\tau},\tau) = (1-\epsilon)Q_{injected}(\tau) \tag{9}$$

This definition is not trivial because the subsurface temperature field is dependent on the ground thermal characteristics as well as the boundary conditions assumed in the heat transfer model. Specifically, in this study, due to variations in groundwater flow field no consistent solution to Eq. 9 can be found that represents the storage domain in all scenarios described in section 3.5. This concern was circumvented, however, by choosing the model setup used for simulation of the pure conduction scenario for defining the storage domain. Calculating the temperature distribution based on pure conduction heat transfer is a sensible choice because it provides possibility to characterize the additional effect of advection on heat flow rates across the storage boundaries.

A discrete approximate approach to the analytical one suggested by (Lazzarotto et al., 2020) was used to define the storage domain $\Omega_{\epsilon,\tau}$. Instead of imposing a transient temperature BC on the BHE array inlets, a constant heat injection power BC were set to each individual BHE for a simulation time duration τ of 180 days. Applying a fraction ϵ of 0.01, the boundary Γ of the storage domain $\Omega_{\epsilon,\tau}$ was determined by finding an approximate minimum of the objective function f_{τ,q_Γ} with respect to the energy density q_Γ at Γ (using T_0 as reference temperature):

$$f_{\tau,q_\Gamma} = (1-\epsilon)Q_{injected,\tau} - \sum_{i\in N} V_i q_i \tag{10}$$

where N is a set of finite elements within the model domain, with energy density q that fulfils the condition $q \geq q_\Gamma$ at time τ. Thus, Γ represents the boundary that encloses the elements in the set N corresponding to the minimum of f_{τ,q_Γ}. The storage domain $\Omega_{\epsilon,\tau}$ is shown in Figure 7.

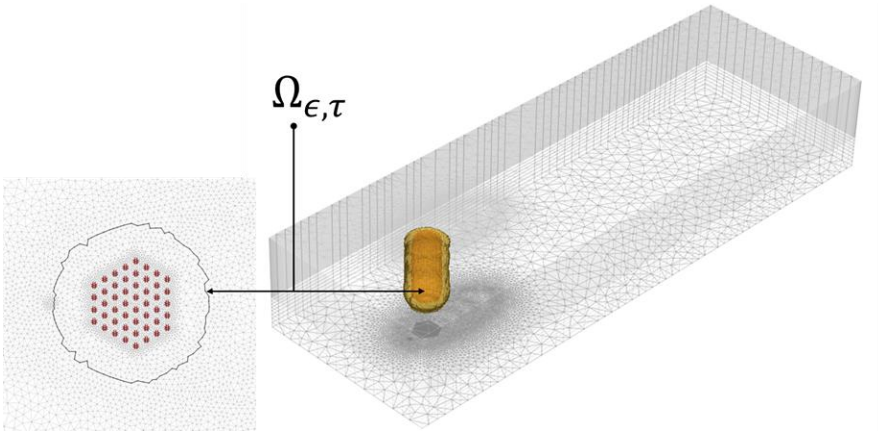

Figure 7. Storage domain $\Omega_{\epsilon,\tau}$ evaluated at time τ =180 days for $\epsilon = 0.01$.

Based on the storage domain $\Omega_{\epsilon,\tau}$, the average storage temperature $\bar{T}_{storage}$ can be estimated by the expression

$$\bar{T}_{storage}(t) = T_0 + \frac{\sum_{i\in\Omega_{\epsilon,\tau}} V_i q_i(t)}{\sum_{i\in\Omega_{\epsilon,\tau}} (V\rho c_p)_i} \tag{11}$$

The system and storage performance indicators presented in Eq. 5-Eq. 8 and Eq. 11 were evaluated for each of the simulation scenarios summarized in Table 4 (section 3.5). In addition, the simulation results were analyzed qualitatively for characterization of mechanisms contributing to heat losses and exergy destruction

during the storage cycle. For defining the integration limits in Eq. 5 - Eq. 6, charging and discharging periods as shown in Table 5 have been considered.

Table 5. Charging and discharging periods.

	Storing cycle 1	**Storing cycle 2**	**Storing cycle 3**	**Storing cycle 4**
Charging period [d]	0-105	370-467	730-828	1137-1189
Discharging period [d]	106-369	468-729	829-1136	1190-1452

4 Results

The results from the simulations of the pure conduction and coupled groundwater flow and heat transport scenarios described in subsections 3.4 and 3.5 are presented in this section. In section 4.1 the outcome of the validation study is presented, which was performed with respect to observed operational and soil temperature measurement data from the Brædstrup HT-BTES to assess the accuracy of the pure conduction model in combination with the plugin tool for BHE array modeling developed within this work (section 3.3). In section 4.2, results are presented for the simulations concerning groundwater advection as well as pure conduction scenarios, in terms of the performance indicators detailed in section 3.6. A qualitative assessment of the importance of groundwater flow on heat loss and exergy destruction events occurring during the storing cycles is given in section 4.3.

4.1 Validation study

The pure conduction model was simulated using aggregated input time series of flow rate, inlet temperature and flow direction (section 3.2) based on real operational data of the Brædstrup storage, considering a time period from 2012-05-22 (start of operation) to 2016-12-31. In Figure 8, computed values of net amount of injected heat, average heat load as well as return temperatures are shown with corresponding observed quantities. All values are aggregated to 72 h resolution, as is the resolution of input time series.

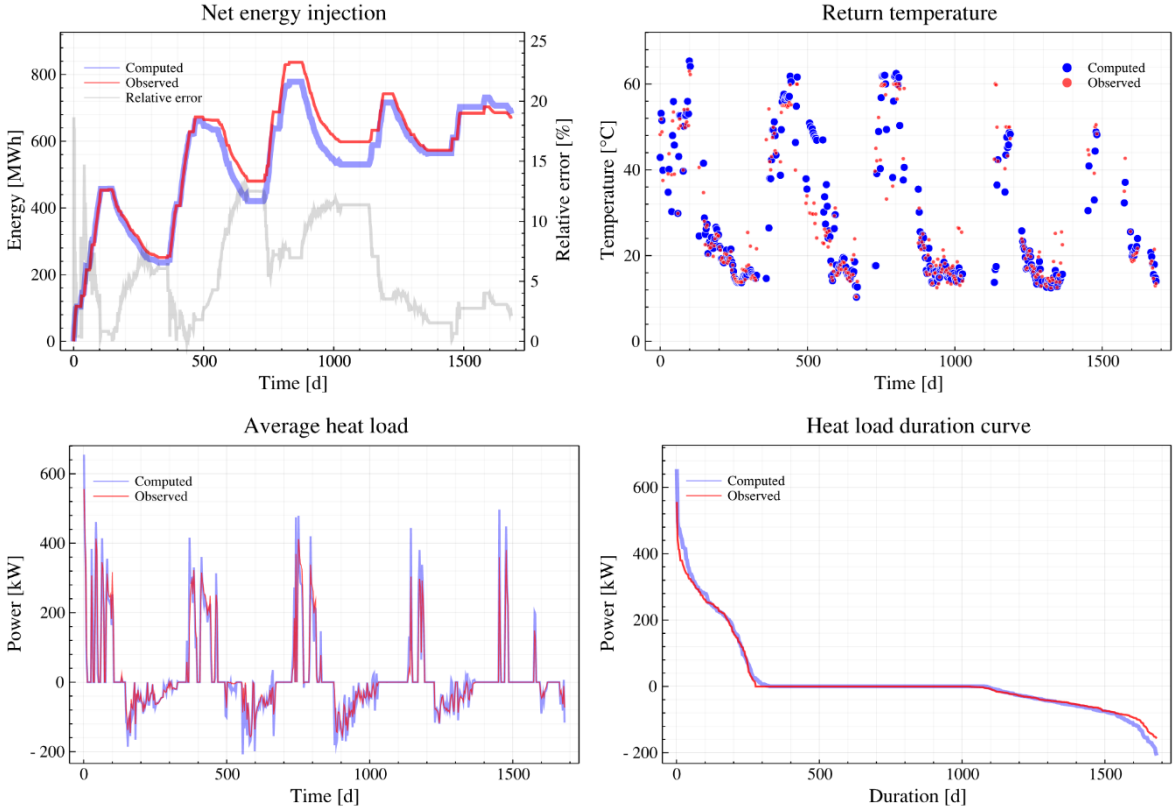

Figure 8. Time series of computed and observed quantities aggregated to a resolution of 72 h. Top, left to right: 1. Net amount of thermal energy injected into the storage. 2. BTES (mixed flow) return temperature. Bottom, left to right: 1. Average heat load on the BTES. 2. Average heat load duration curve.

As can be seen in Figure 8 (top, left), computed values of net injected heat show good agreement with observed data, particularly at times during the first charging period but also during the second charging period. Some divergence can be observed during the first discharging season, which is a tendency that reappears also for subsequent discharging periods. This tendency was also observed by (K. W. Tordrup et al., 2017), who suggest that the deviation may be due to the BHE model used (Eskilson and Claesson, 1988) being inaccurate for highly transient loading conditions, as it assumes quasi-stationary behaviour of the BHE. Consequently, simulated BTES outlet temperatures will deviate from real values. Such an example can be seen in Figure 8 (top, right) during the second discharge period, where overestimations in computed

return temperatures introduce an offset of about 55 MWh during the subsequent storing cycle. Considering such tendency in combination with the approximate method used for linking the BHE outlets/inlets in the BHE array modeling plugin, care must be taken when applying the tool for short-term problems. However, as indicated by the relative error indicator shown in the energy chart (top, left), the deviation decreases during the fourth storing cycle and the relative error reduces to around 2% (682 MWh computed vs 668 MWh observed net energy injection into the storage) at the final time step of the simulation. In Table 6, a summary of other basic measures of errors between computed and observed data is presented.

Table 6. Basic measures of errors between computed and observed data.

	Net injected energy [MWh]	**Power [kW]**	**Return temperature [°C]**
RMSE	40	29	7
Maximum absolute error	77	250	43.3
Max. (computed/observed)	778/836	655/556	65.4/63.0
Min. (computed/observed)	0/0	-208/-156	10.3/10.4

For assessing the soil temperature prediction ability of the pure conduction model, temperature simulation results were recorded at 3D locations corresponding to those of the actual temperature probes inserted in observation wells T1-T5 (see Figure 1 in section 3.1) and evaluated by visual comparison with observed data. Observation wells T1, T2, T3 and T5 are located inside the external circumference of the bore field, whereas T4 is located at ~11 m from the bore field periphery. Time series records of computed and observed soil temperatures at 15 different points are shown in Figure 9. Here, three depths for each of the observation wells have been randomly selected to reflect the overall tendencies of the model prediction capabilities.

Computed temperatures generally agree well with observed soil temperature data. However, the model seems to overestimate near-surface soil temperatures, especially during times when the BTES system is inactive (e.g., T2 at 3 m and 4 m; T3 at 1 m; T5 at 2 m), which is possibly due the assumption of adiabatic ground surface at the top boundary of the model domain. Outside the bore field and beneath the BHEs, the model generally fails to accurately capture the dynamics of the soil temperature pulses occurring during the storing cycles (e.g., T3 at 50 m; T4 at 9 m; T5 at 51 m), although temporal-averaged time series of the temperature data would show reasonable accuracy. Inside the bore field, at intermediate depths relative the length of the BHEs (e.g., T1 at 19 m; T2 at 24 m; T3 at 14 m), very good agreement can be observed between computed and observed data considering the high and rapid variations in temperature levels occurring over the course of a storing cycle. It can be seen that the model is also capable of capturing thermal stratification within the storage by noting that the highest computed and observed overall temperature levels are reached in T5 (T5 at 2 m and 9 m in Figure 9), which is the innermost of the five observation wells in relation to the storage center.

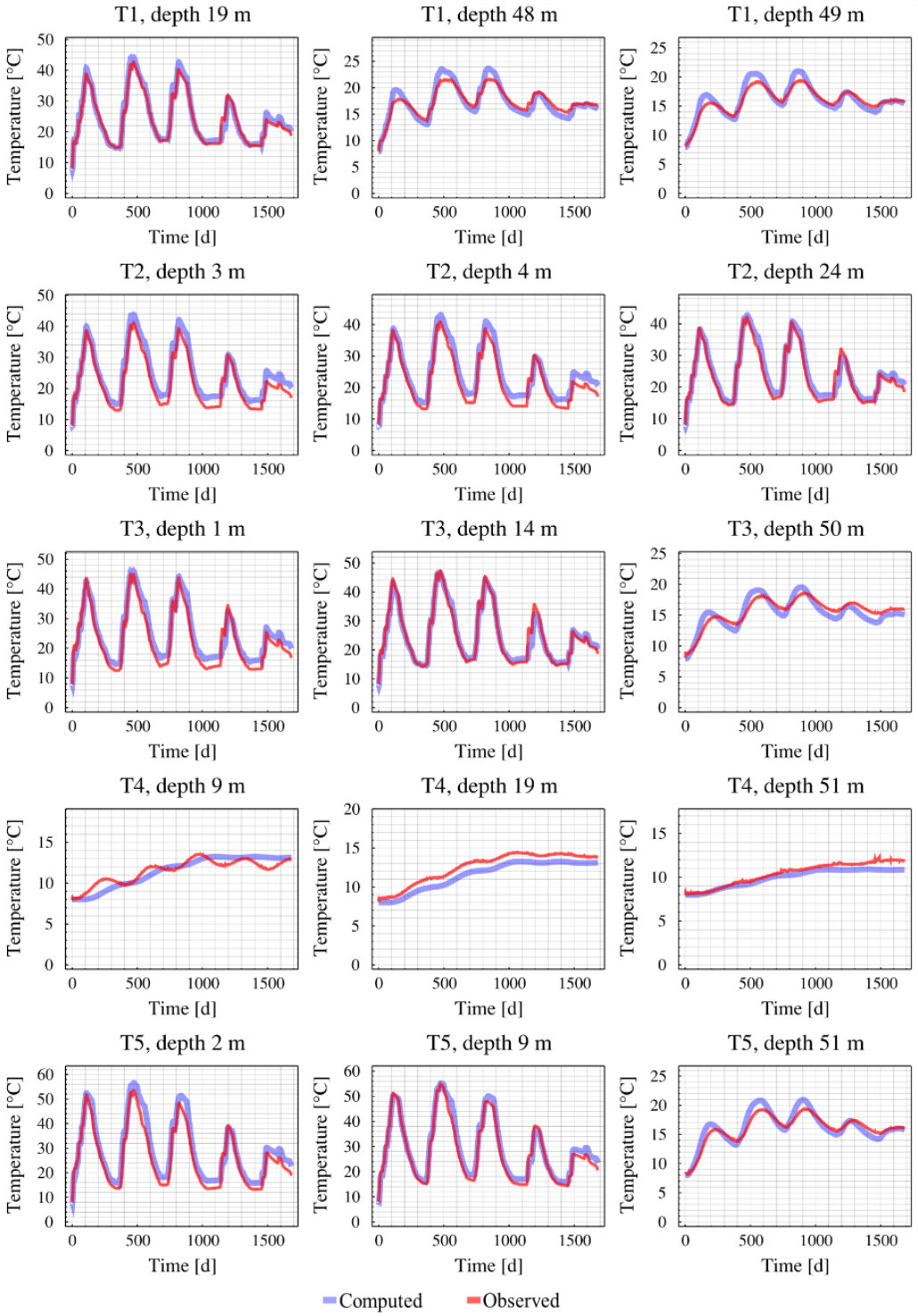

Figure 9. Time series records of computed and observed soil temperatures at 15 different points.

4.2 Energy and exergy performance indicators

Storage performance and system seasonal performance were evaluated in terms of energy and exergy efficiency in accordance with the definitions given in section 3.6. Figure 10 shows the results in terms of seasonal system performance indicators. First, a note must be made on the seasonal development of the indicator values. Comparisons between different storing cycles must be made with caution since the flow rate and BTES forward temperature vary over the seasons, which has direct impact on the amounts of energy and exergy exchanged during each cycle. However, it can be seen that scenarios concerning pure conduction (S1) and hydraulic head difference of 1 m across the model domain (S2) show quite similar performance in seasonal energy exchange and efficiency for each storing cycle. During the fourth storing cycle, S2 even performs slightly better than S1 in terms of energy efficiency. This may be attributed to enhanced heat transport within the storage due the groundwater movements, and similar tendency was observed by (Bauer et al., 2009) in their study on the performance of a high temperature BTES. For the scenarios concerning higher hydraulic head differences (S3, S4, S5), detrimental effects on the storage energy efficiency become evident as their indicator values decreases with increasing hydraulic head for each cycle of operation. It can also be observed that higher groundwater flow rates consistently tend to contribute to higher charged energy and less discharged energy amounts.

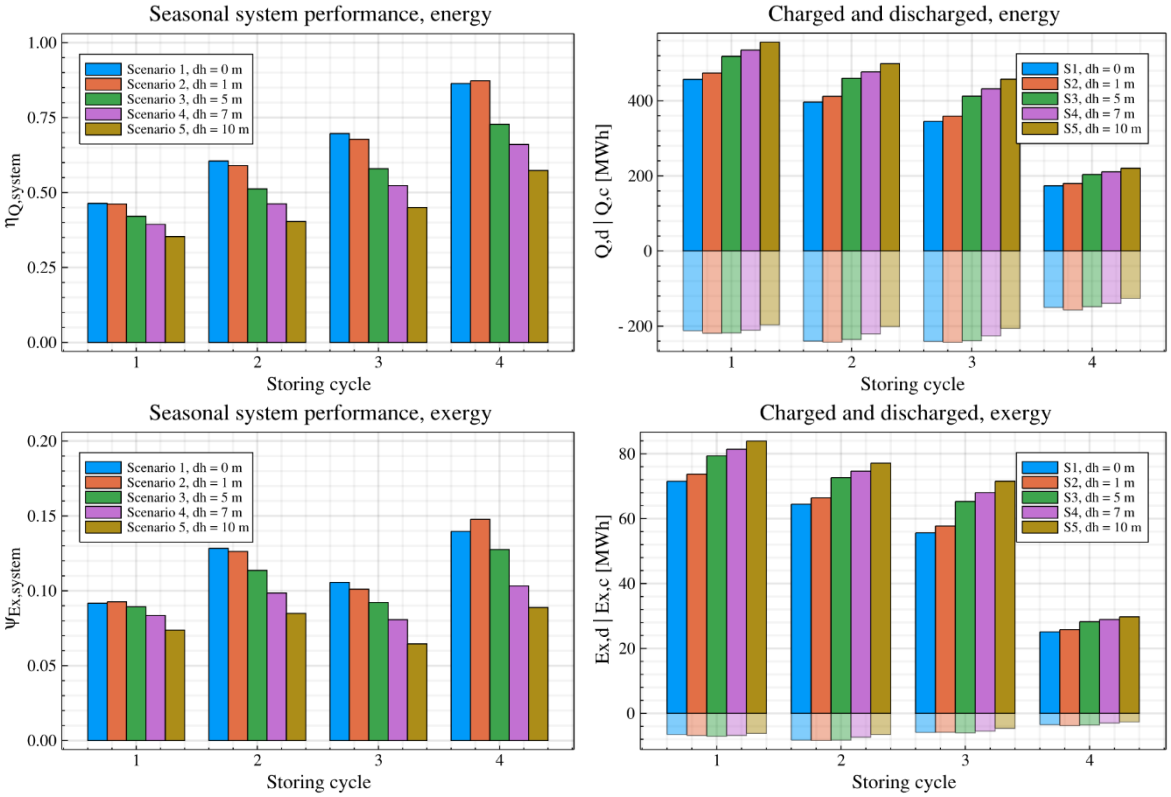

Figure 10. Left: Seasonal energy efficiency ($\eta_{Q,system}$) and seasonal exergy efficiency ($\psi_{Ex,system}$) computed for the first four storing cycles.

Similar trends can be distinguished concerning seasonal exergy efficiencies shown in Figure 10 (bottom charts). However, during the second storing cycle all exergy efficiency indicator values of each scenario differ positively from those evaluated during first and third storing cycle. This is an effect caused by initially high estimated return temperatures during discharge, which is clarified in Figure 11 (top), showing forward and return temperatures for all scenarios during the charging and discharging periods. It is worth to note that return temperatures during this period tend to be overestimated as compared to observed data (see

section 4.1), although the figures depicted here only consider modeled scenarios with identical conditions besides the hydraulic head value imposed on the upstream boundary.

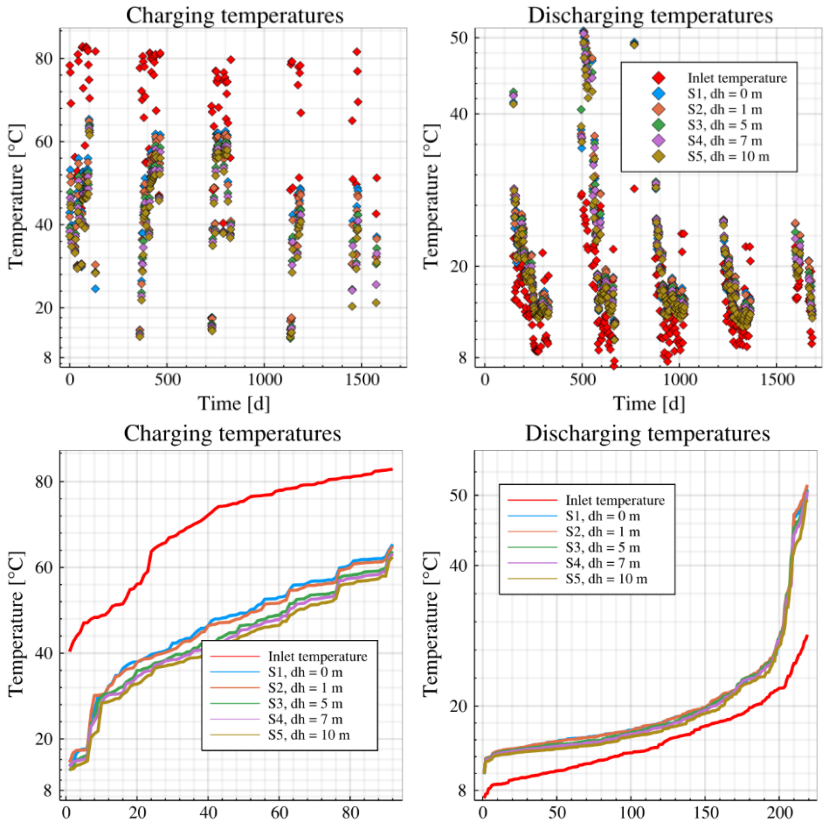

Figure 11. Top, left to right: 1. Charging temperatures vs. operation time. 2. Discharging temperatures vs. operation time. Bottom, left to right: 1. Duration curves for inlet and outlet temperatures during charging operation. 2. Duration curves for inlet and outlet temperatures during discharging operation.

Another observation from Figure 10 is that charged amounts of exergy tend to deviate more than discharged exergy amounts when comparing the scenarios for single storing cycles. For clarity, charging and discharging temperatures are presented sorted in ascending order in Figure 11 (bottom), where the horizontal axes represent the number of data points with 72-h resolution. While there is a clear difference in overall charging return temperature levels between the scenarios, less deviation can be observed between the sorted values of discharging return temperature. This is an indication that groundwater flow tends to enhance exergy exchange during charging, but it is not the dominating mechanism of degradation of the temperature build-up within the storage after charging ends, for the specific groundwater flow rates, storage design and operation conditions considered.

This is further shown by observing storage energy and exergy performance indicators seen in Figure 12. Apparently, differences between the scenarios tend to be more pronounced when regarding energy storage performance. It is seen that groundwater flow has a clear effect on the net amount of energy injected into the ground, which is primarily driven by enhanced exchange rates during charging, and less importantly by differences in discharging heat rates. For the initial storing cycles, higher or similar amounts of energy are stored within the storage when comparing groundwater flow scenarios with the pure conduction case, indicating that additional heat flow across storage boundaries induced by advection is rather balanced with the additional heat injection. This tendency does however decline as time develops, and at the final time step the largest amounts of stored energy are observed for the scenarios considering no (S1) or low (S2) groundwater flow velocities, although these scenarios show the lowest amounts of net energy injected. Consequently, as the increase of groundwater velocity, storage energy efficiencies are decreasing after a

certain time. At the end of the simulation period, the storage energy efficiency for the case of highest velocity (S5) is 18%, as compared to 45% in case of pure conduction (S1).

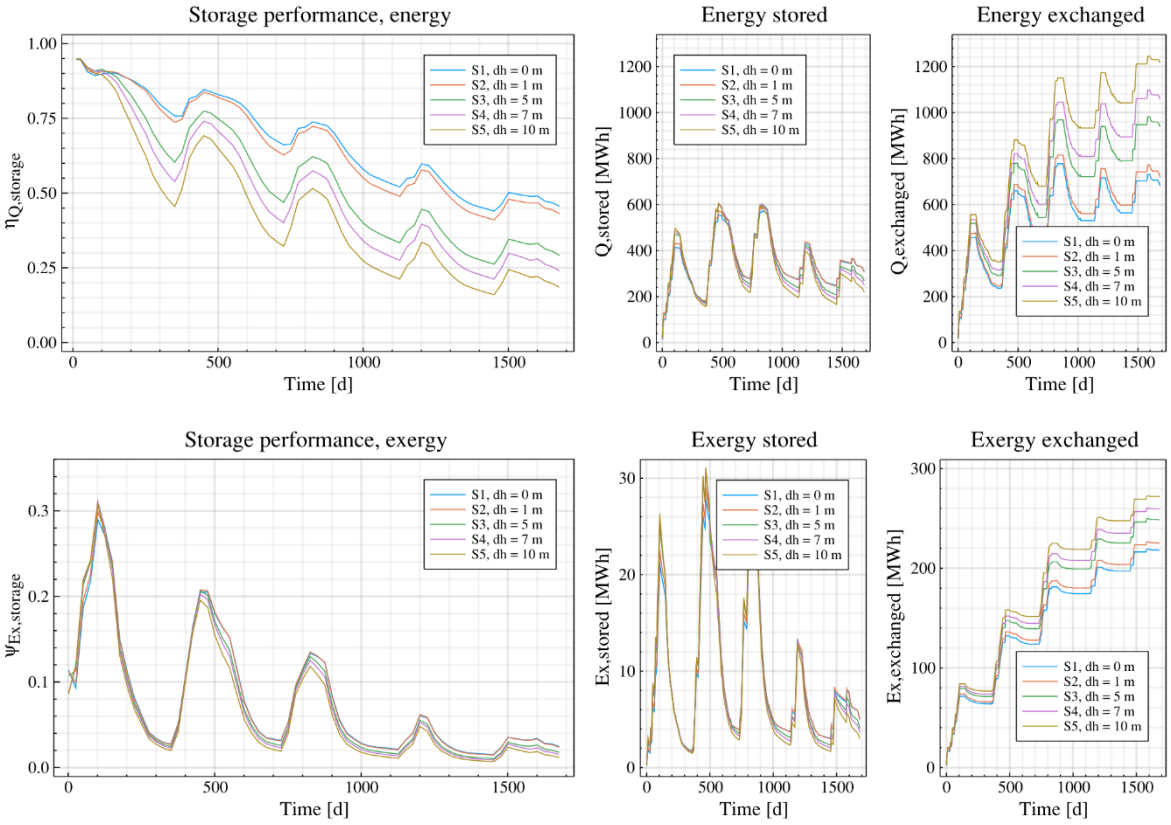

Figure 12. Storage energy efficiency ($\eta_{Q,storage}$) and storage exergy efficiency ($\psi_{Ex,storage}$).

By comparing the plots showing energy and exergy storage efficiencies in Figure 12, it appears that the exergy indicator is less sensitive to groundwater flow rate than the energy indicator. Again, as in the case of energy exchange, it is evident that groundwater flow promotes exergy transfer during charging. It can also be seen that the amount of exergy extracted from the storage is rather low and equal for all scenarios, but this tendency is not reflected by the figure representing the amount of exergy stored in the storage volume, which still shows large fluctuations between charging and discharging periods as a result of exergy losses and destruction. For example, at the end of the initial charging period around 70% of the exergy injected into the storage was already lost or destroyed in all scenarios. During the subsequent discharging period, only around 6 MWh of exergy was extracted, while the amount of exergy stored dropped from between 20-24 MWh to less than 2 MWh at the end of the storing cycle irrespective of groundwater flow rate. Hence, there is a single or combination of mechanism that causes large exergy loss and destruction rates within the storage volume, and the exergy storage performance is accordingly poor. Although it can be seen after a couple of storage cycles that lower groundwater flow velocities contribute to somewhat higher exergy storage efficiency, it is not of main importance for the overall performance. It should, however, be noted that the effect of groundwater flow on exergy performance could be more prominent under other operation and subsurface conditions than the ones set out in this study.

As can be understood from the definitions of the storage energy and exergy performance indicators (section 3.6), exergy analysis is capable of reflecting the quality of the heat being injected, stored and extracted, which is in contrast to energy analysis that only considers quantity. In the case of the Brædstrup HT-BTES, the system is operated using rather high charging temperatures (i.e. high quality heat), while heat is discharged at temperatures relatively close to the reference environment (undisturbed ground) temperature (Figure 11). Under such conditions energy extraction is promoted and the storage temperatures will be kept at moderate levels (see Figure 13), but the exergy performance will be penalized.

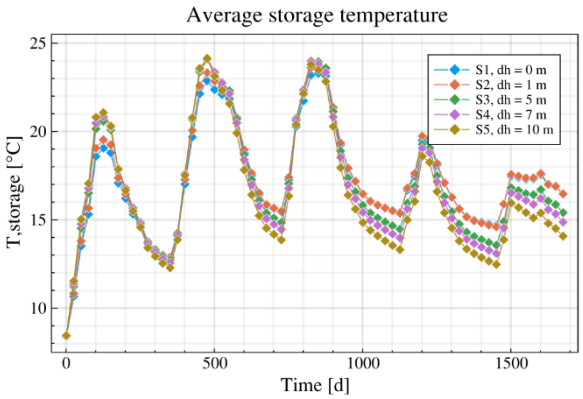

Figure 13. Average soil temperature inside the storage domain.

In this view, an alternate operation strategy could for example be to use the high quality heat for short-term storage purposes and use lower quality heat to balance a combined heat and cold storage operating alternately above and below the temperature of the undisturbed ground. Otherwise, the high quality heat could be used to maximize the temperature build-up within the storage, in combination with energy extraction rate control with respect to a threshold discharge temperature that enables the heat to be recovered possibly without the use of heat pumps. In the latter case, the effect of groundwater flow on exergy storage would probably be relatively more prominent because of cold groundwater is advected into the storage region and contributes to temperature degradation by mixing and disturbance of stratification. For a storage operating under balanced conditions at temperature levels close to the undisturbed ground temperature, this effect is expected to be minor.

4.3 Energy losses and exergy destruction

Temperature fields obtained from the simulations were visualized to provide a qualitative insight on groundwater impacts on storage thermal performance. For this purpose, the scenarios concerning minimum (S1) and maximum (S5) groundwater velocity were considered to demonstrate the contrast between pure conduction and advection-influenced conditions. The relative importance of advective to conductive heat transport can be expressed by a dimensionless parameter called the Péclet number, which characterizes the ratio of the heat advection rate caused by groundwater movements to the rate of temperature gradient driven heat conduction:

$$\mathrm{Pe} = \frac{Lq}{\alpha} \tag{12}$$

where L is a characteristic length, here the borehole length, q is the Darcy flux and α is the thermal diffusivity of the porous medium. As shown in Figure 14, the Darcy flux varies greatly over low- and high-permeability layers for the groundwater flow scenarios, and the Péclet number is varying accordingly. For Péclet numbers greater than 1, advective transport dominates over conductive effects. This is true in the depth intervals of 9-20 m and 26-80 m for all flow scenarios except S2, where Péclet numbers larger than unity are reached only in the interval of 26-41 m. In the low-permeability zones Péclet numbers are several orders of magnitude smaller than 1, thus a conduction-dominated thermal regime prevails in these layers.

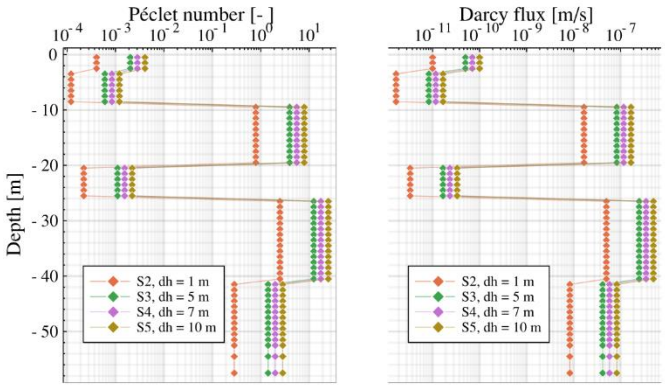

Figure 14. Variation of Péclet number and Darcy flux with depth.

For scenario S5, Péclet numbers in the range between 1.2E-3 and 2.5E+1 are obtained, corresponding to Darcy flux rates between 1.7E-11 m/s (1.44E-4 cm/d) and 5.0E-7 m/s (4.3 cm/d). Considering these rates relative to the spatial and temporal scale of the storage and the storing cycles, respectively, only flux rates having similar magnitudes as the latter are expected to be high enough to have visible impact on the temperature distribution over the course of a storage cycle. In Figure 14, cross-section views of the storage visualizing the evolution of the temperature distribution (described by combined continuous temperature and isotherms plots) during the initial storing cycle for scenarios S1 (pure conduction) and S5 (maximum hydraulic gradient) are shown.

The times considered here correspond to the end of the charging period (105 d), 12 days ahead of discharging start (135 d), 3 days after discharging start (150 d), and subsequent times (201 d, 249 d) until end of the initial discharging period (369 d). The storage domain is indicated as a fixed line surrounding the BHEs. Indeed, groundwater flow effects on the thermal distribution can be observed within the high-permeability zones already at the end of the charging period. These effects appear as thermal plumes that develop in the downstream direction of the flow. It can also be seen that the thermal distributions within the low-permeability zones are initially similar for both scenarios. The storage in both scenarios exhibits temperatures equal to or larger than 54 °C at the center regions, but this high temperature field is considerably more developed in the groundwater flow scenario due to heat transfer enhancement effects. Some tendency of the high temperature field being displaced in the direction of the groundwater flow can be observed, although the highest thermal energy density still is concentrated close to the storage center. The visualizations comply well with the quantitative results presented in section 4.2, where stored amounts of energy and exergy as well as average storage temperature are shown to be at highest levels for the case of maximum flow rate at the end of the initial charging period.

At time 135 d, the storage is in inactive operation mode before discharging starts at time 147 d, hence any changes in storage energy or exergy content are due to subsurface losses or destruction. Comparing the temperature fields at 105 d and 135 d clearly shows that a main part of the region containing high quality heat (≥ 54 °C) have been degraded in both scenarios. The rapid rate of temperature loss also in scenario S1 indicates that heat conduction is a significant source of exergy destruction during this phase. Advective effects on the center region temperature field also become more prominent. A clear disturbance of the temperature field particularly in the lower high-permeability layer can be observed, which results in locally lower ground temperatures close to the BHEs located in the upstream region of the storage, and vice versa in the downstream region. While no substantial heat flow across the storage boundaries can be seen in the pure conduction scenario, temperatures up to around 28 °C occur outside the storage domain at time 135 d.

The plots showing temperature fields at consequent times (150-369 d) represent the development of the thermal process occurring during discharge. The presence of BHEs is indicated by slender vertical low temperature regions inside the storage. Shortly after discharging starts (150 d), clear horizontal stratification and uniformly distributed thermal gradients can be distinguished in the pure conduction scenario, which enable efficient use of the series connected BHEs.

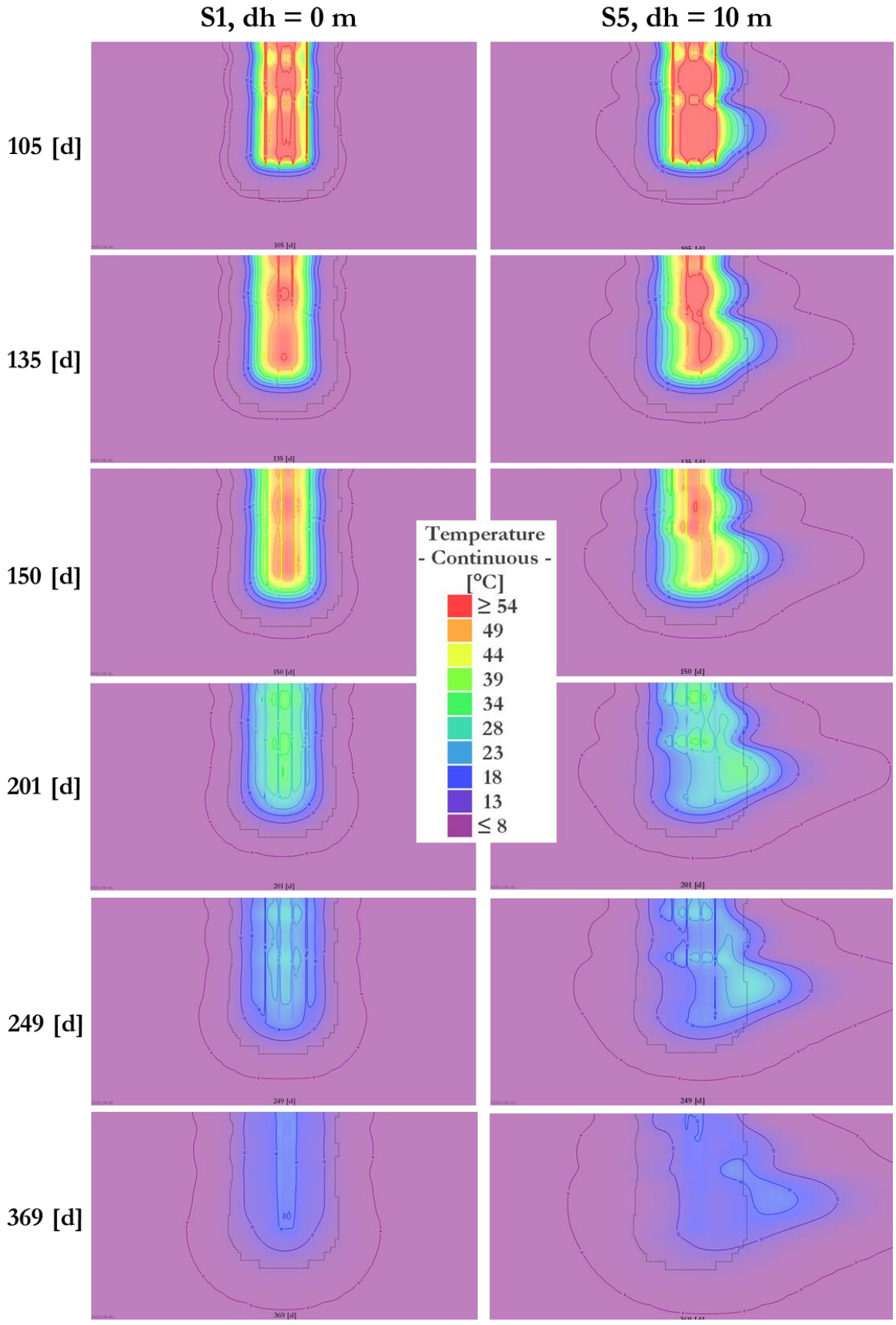

Figure 15. Cross-section views of the storage showing the evolution of the temperature distribution during the initial storing cycle for Scenario 1 (pure conduction) and Scenario 5 (maximum hydraulic gradient).

This is not the case in the groundwater flow scenario, where a distorted and, locally, a slightly layered temperature distribution has been induced. A possible consequence of this effect might be, for example,

that the heat carrier fluid extracts heat in one region of the storage domain and re-injects it into another region at lower temperature. Depending on storage temperature distribution and BHE array arrangement, this could possibly even result in net energy injection into the storage through some of the BHE arrays, contrary to the intended discharging operation.

During remaining times (201-369 d), the temperature build-up within the storage continues to degrade. At final time, it can be clearly seen that large amounts of heat have been lost to the ambient ground in the groundwater flow scenario. The heat that has been advected downstream the storage region cannot be recovered. As shown in section 4.2 (Figure 12), only ~45% of the net injected heat remains within the storage domain at the end of the first storing cycle, as compared to ~75% in case of the pure conduction scenario.

Another view of the storage at identical times as those considered above is shown in Figure 15. Here, horizontal temperature fields at a depth of 35 m are shown in relation to BHE locations and BHE array arrangement, allowing for better demonstration of the importance of thermal stratification within the storage. As can be seen at time 150 d, a drift of the high temperature region originating from the storage center can be identified in the groundwater flow scenario. Because of the advection movement, only a single (out of eight) array outlet borehole intersects with the region defined by the maximum isotherm shown (49 °C) at this depth. At the subsequent time point, the maximum isotherm has decreased to 28 °C, and the region within this contour is completely located outside the bore field perimeter. This implies that no efficient storage operation and use of the heat injected can be accomplished under these conditions, with the specific borehole arrangement considered.

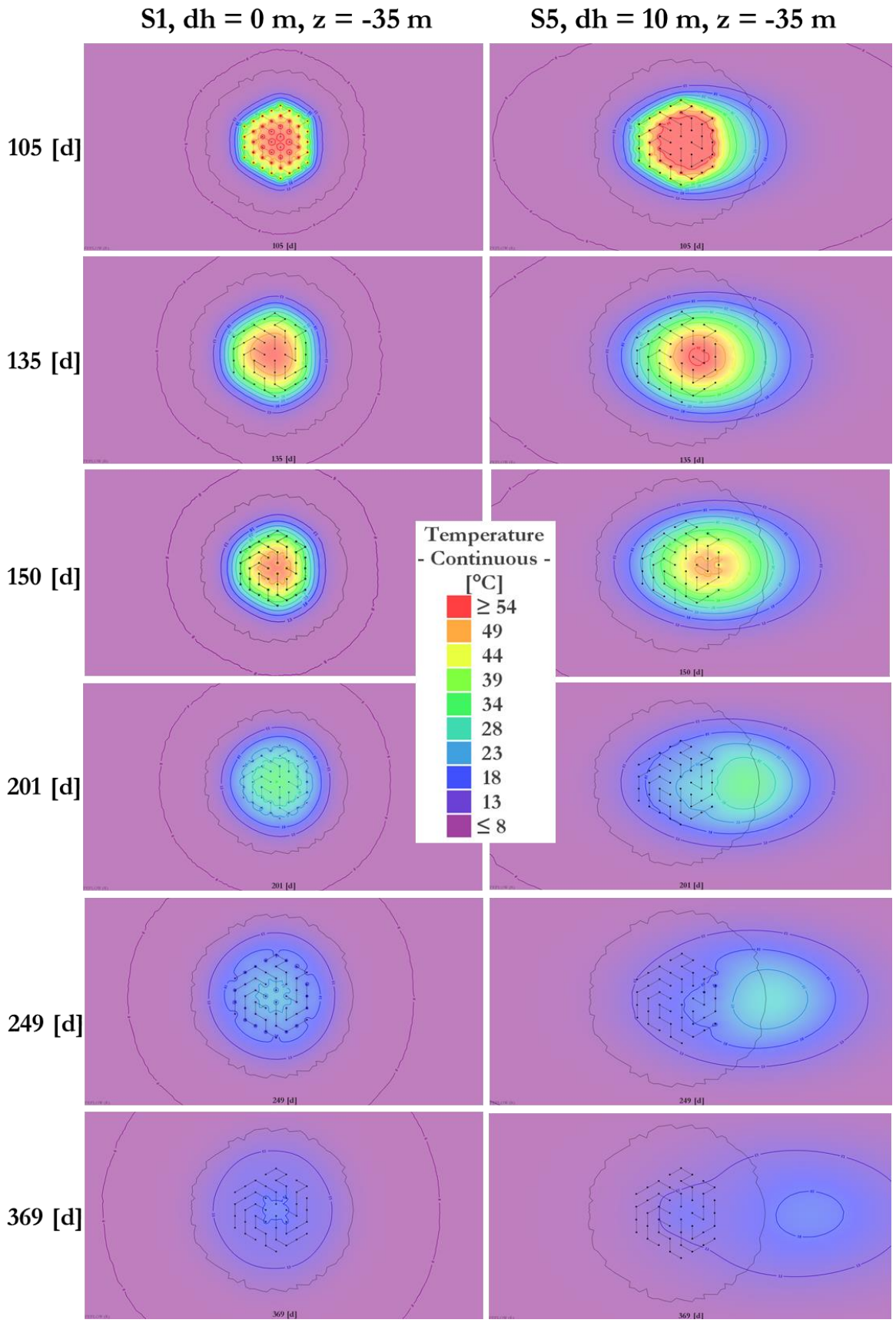

Figure 16. Top views of the storage at z = -35 m showing the horizontal temperature distribution development during the initial storing cycle for Scenario 1 (pure conduction) and Scenario 5 (maximum hydraulic gradient).

5 Discussion

Development of efficient borehole thermal storage systems requires profound understanding of the subsurface thermal and hydraulic processes involved, as well as of the importance of proper operation strategies and BHE designs. Detailed and accurate coupled hydro-thermal modeling of subsurface processes could greatly help to gain insight into BTES thermal behavior under different ground conditions. Coupling between models of the BTES and other components within an energy system would also allow for advanced prediction and optimization procedures to be implemented in system design and operation.

Modeling of coupled subsurface processes is however associated with many challenges, which bring considerable difficulties to BTES thermal analysis. Among them, ground heterogeneity, anisotropy and scale effects can particularly be sources of difficulties in characterizing ground conditions and accurate modeling of subsurface thermal distribution in BTES systems. This is particularly true in fractured hard rock environments, where the fluid flow behavior commonly is significantly affected by intrinsic variety of fracture network characteristics at different spatial scales. Increasing development of underground infrastructure as well as conflicting interests in subsurface resources, especially in urban areas, are also factors likely to add complexity to the problem. Not only could groundwater aspects be of importance for BTES design and performance, but they could also be of significance regarding BTES thermal and chemical impacts on the surrounding environment, which may be more sensitive to groundwater movements than the storage itself. Hence, there is a need for gaining a deeper understanding of how BTES and groundwater systems interact, and what possible impacts that could follow in different environments.

Although groundwater aspects have received relatively little attention in research in closed-loop shallow geothermal systems, concepts of groundwater flow and subsurface transport processes have been extensively studied within the field of hydrogeology and other geosciences disciplines during the last decades. Significant advancements have been made in understanding these processes for a wide variety of hydrogeological conditions. Approaches for dealing with even extreme heterogeneity and anisotropy (e.g., in the case of fractured hard rock) have been developed, driven among other by extensive research programs on nuclear waste disposal in deep rock repositories.

Although being applicable to other problems, e.g., thermal storage in shallow fractured rock, assessment of what approach is best suited for the specific application, the spatiotemporal scale of the problem, the ground characteristics, and the level of accuracy and detail required is not trivial. First, there is a paucity of experimental data regarding BTES subsurface temperatures in general, and particularly from systems in groundwater rich areas or in fractured rock. Second, adoption of modeling approaches employed for other engineering applications and research disciplines (e.g., enhanced geothermal systems, CO_2 sequestration, waste disposal etc.) must be done with care, since the spatial or temporal scale or other aspects of the processes involved could be fundamentally different. Third, the characteristics of a flow and transport problem are often very site-specific, and the validity of a specific modeling approach must be assessed within that context. For example, employing the classical continuum modeling approach to study flow and transport processes within a granular porous material is most often a reasonable choice, while in a fractured rock mass for which a representative elementary volume cannot be found it would not be meaningful. Instead the actual geometry of the water-bearing features must be considered to some extent (see, e.g., (Shapiro, 1987)). Validation and applicability assessment of conceptual or mathematical modeling approaches available is thus not straightforward, and a generic answer to the question of what approach that is best suited for handling flow and heat transport processes in BTES systems cannot be given. An elaboration on these issues is given by (Tsang, 1990).

To make further advancement in understanding coupled hydro-thermal processes in BTES applications, efforts related to the issues discussed above should be made. A key contribution could come from experimental data, which requires further implementation of pilot or full-scale BTES projects with focus on designing data acquisition systems that are well suited for monitoring subsurface hydraulic and thermal processes during operation. This also includes development of in-situ investigation methods for combined characterization of hydrogeological and thermal ground conditions (see, e.g., (Klepikova, 2013)), that are capable of capturing characteristics at all scales relevant to the problem. Moreover, a comprehensive review

and comparison of concepts and methods used to study groundwater flow and transport processes in porous and fractured media (in particular) could be carried out, and their applicability in the context of BTES modeling could be assessed. Both implicit as well as explicit conceptual and numerical models for representing fractured porous media (Berkowitz, 2002; Berre et al., 2018) should be employed and compared. Detailed analysis would provide deeper intuitive and computational understanding of how observations made of in-situ hydraulic and geometric fracture characteristics translate to predictive ability. That is, to gain an understanding of at what critical level of fracturing etc. advection effects might become significant to BTES thermal performance. Also, detailed modelling using explicit conceptualizations of water-bearing features can be an effective approach for assessing the accuracy and applicability of less computationally demanding implicit models (see, e.g., (Chen et al., 2017)).

Besides the importance of accurately considering the hydro-thermal processes occurring in the ground, a detailed and realistic representation of the ground-coupled heat exchanger system is required to enable precise evaluation and optimization of the thermal performance of the BTES. The great variability in possible BHE arrangements and operation strategies, associated with the objective of maintaining thermal stratification within a HT-BTES, entails more modeling complexity when compared to ordinary parallel-connection arrangements that are frequently used in low-temperature systems. The FEFLOW plugin tool developed within this work (Section 3.3) allows for modelling of any number of arbitrarily interconnected BHEs. Currently, the plugin supports boundary conditions with equal array inlet temperature and flow rate, and variable flow direction according to user-defined control rules. Further efforts can be made to extend the modeling capabilities by implementing support for other types of BHE boundary conditions as well as coupling with dynamic energy simulation codes such as TRNSYS or Modelica-based software to model the interaction between the BTES and other components within the energy system.

In the validation study (Section 4.1), it was found that the pure conduction model could fairly accurately reproduce observed BHE heat exchange rates as well as depth-distributed soil temperatures measured at different locations throughout the Brædstrup storage. Hence, the FEFLOW plugin proved to be a useful tool for predicting the thermal behavior of the BHEs and capturing the thermal dynamics of the storage, including the thermal stratification that is built up due to the series-connection BHE arrangement used in the BTES design. These are important features for evaluating the thermal performance of the BTES and thus, their accurate prediction gives the possibility to optimize the design and operation of the storage with regards to for example energy or exergy efficiency. However, it must be emphasized that the plugin has shown to be valid only for this specific model, and hence further validation with other BHE geometries, series arrangements, input data time resolutions etc. is required. A limitation of the numerical approach employed in this study is that the computational burden of the calculation can be very high compared to analytical methods, especially in cases when high temporal resolution of boundary conditions or dependent variables is required. A temporal resolution in the order of days, as was applied in this study, can be adequate for capturing the thermal dynamics of the ground, but for predicting the short-term behavior of the BHEs it is not suitable. Substantial computational effort can however be saved by the use of the quasi-stationary analytical BHE model by (Eskilson and Claesson, 1988) available in FEFLOW. It comprises a reasonable compromise between computational efficiency and accuracy, and has shown to be a good alternative to numerical 1D BHE models as well as fully discretized 3D solutions for processes occurring at temporal scales larger than a few hours (DHI-WASY, 2010). Because of the assumption of local steady-state conditions inside the BHEs, care must though be taken if the actual short-term loading conditions are highly transient. This was the case especially during the discharge periods, which consequently contributed to deviations between observed and computed BHE temperatures. These tendencies were also reported by (K. W. Tordrup et al., 2017).

Overall, however, the agreement between computed and observed heat exchange rates and subsurface temperature is fairly satisfactory. The temperature fields obtained from the simulation of the pure conduction model can therefore be considered to be suitable for analyzing the thermal behavior of the real storage, as well as for comparisons with simulation results obtained from other models accounting for alternative hypothetical loading or ground conditions. In this work, the pure conduction model served the purpose of providing a reference scenario for evaluating how the storage performance depends on

groundwater flow under equal charging and discharging (flow and inlet temperature) conditions. Although a simple, hypothetical representation of a real groundwater system, the coupled hydro-thermal model features some characteristics that may be encountered in many hydrogeological environments. For example, vertical soil heterogeneity was accounted for by assigning a hydraulic conductivity value to each of the geological layers that were identified by (K. W. Tordrup et al., 2017). The presence of highly conductive as well as low-permeability adjacent sublayers creates an extremely heterogeneous environment where both conduction and advection dominated heat transport regions may exist if a hydraulic gradient is present (Figure 14). The variability in thermal regimes between these regions suggests that considering solely heat conduction or assuming homogeneous medium, which are common assumptions in design of closed-loop shallow geothermal systems, may in some cases be insufficient to provide a good representation of the processes that occur in the actual system. Therefore, when investigating a potential storage site or designing the borefield, it is of importance to consider the site-specific conditions and collect appropriate information to assess the validity and applicability of these assumptions.

By extending the performance evaluation analysis beyond the boundaries at the BHE inlets and outlets, it is possible to compare quantitatively how different subsurface characteristics affect the storage capacity and the temperature regime inside the storage. There are some limitations associated with the conventional seasonal energy efficiency/utilization ratio indicator that is frequently used in the literature to assess the performance of BTES systems. To evaluate this performance figure, the storage is essentially treated as a black-box system without considering neither how energy is lost nor how it is charged and discharged. For example, it is possible to achieve a seasonal energy ratio of 1 if heat is discharged at temperatures lower than that of the undisturbed ground (e.g., in the case of BHEs coupled to a heat pump), but the discharge rate of the same storage could also be restricted due to temperature mismatches if the system is directly coupled to the heat sink. Also, no information is provided on how the injected heat is distributed in the ground, e.g., whether it is still available in the vicinity of the BHEs or has been lost to the ambient. Overall, the sole consideration of energy efficiency cannot be deemed sufficient for evaluation of BTES system thermal performance since it does not adequately address concerns about the thermal processes occuring within the storage. Neither does it explicitly account for the temperature at which heat is injected, stored and extracted. Therefore, by introducing the concepts of exergy and storage efficiency in the analysis, a better characterization of the system and storage performances can be achieved. The four indicators employed in this study depict the energy and exergy performance at the system level (based on inlet/outlet quantities) as well as at the storage level (based on inlet/outlet and subsurface quantities). Although each of the indicators alone cannot capture all factors relevant for assessing the thermal performance of the storage system, together they complement each other and provide a rational and comprehensive basis for BTES performance evaluation. However, while the seasonal system indicators have been fairly established in the literature (e.g., (Kizilkan and Dincer, 2012; Rezaie et al., 2015)), the storage indicators were recently introduced by (Lazzarotto et al., 2020) and are rather novel in BTES applications. Since evaluation of the latter indicators depend on a parameter representing the storage volume, a viable definition and consistent application thereof is required to facilitate comparison of storage performance across studies dealing with different BTES designs and subsurface conditions. Defining the storage volume is not straightforward due to the ambiguity of the lateral and lower boundaries of the storage. In (Lazzarotto et al., 2020) as well as in the present work, the storage volume was defined by identifying a subdomain containing a certain portion of the total amount of heat injected after a characteristic time (see Section 3.6). This approach is not ideal for assessing and comparing storages that are situated in environments with substantially different conditions. If the storage domain is defined using the actual heat distribution it will also reflect and depend on factors contributing to losses and will thus contain a large amount of non-recoverable heat. Considering that the purpose of the storage performance indicator is to quantify the ability of the storage to maintain the injected heat within the storage volume, the limitations of this definition become apparent. Therefore, future work may study how the selection of storage volume affects the storage performance indicator values, and whether other approaches to defining the storage volume might be better suited. For example, a definition of the storage volume based on the geometric characteristics of the BTES can be considered, as is done, e.g., in the DST model (Chapuis and Bernier, 2009). Extending the energy and exergy analyses by considering also smaller subdomains within the storage could help to improve the understanding of the

thermal behavior of the BTES. Likewise, refining the resolution of the analysis at the system level (e.g., by evaluating the performance of individual BHE arrays) may also help to provide better insight in the functioning of the system and to identify sources of inefficiencies throughout the storing cycles.

From the energy and exergy analyses, it was found that groundwater flow has in general negative impact on the BTES thermal performance, which tends to decrease with higher flow rate. This finding is in agreement with most studies that have investigated groundwater flow effects on BTES systems (Catolico et al., 2016; Diersch and Bauer, 2014; Nguyen et al., 2017). A few exceptions to this trend could however be observed. For example, for the case of the smallest non-zero hydraulic gradient considered, it was found that the BTES seasonal energy and exergy efficiencies occasionally were slightly higher when compared to the case of pure conduction. This can possibly be attributed to enhanced heat transfer induced by the groundwater movement. It is, however, likely that after a time longer than the simulation time considered, consistently negative effects of groundwater flow can become apparent also in this scenario. To gain a more thorough understanding of the influence of groundwater flow, parametric analysis considering larger time scales and different ranges of groundwater flow rates as well as charging and discharging temperature levels is recommended. For this purpose, rather than computationally demanding numerical methods, analytical models could provide a suitable means to generate the extensive simulation data required for the analysis.

6 Conclusions and recommendations for future research

The assumption of pure conduction heat transfer in a homogeneous and isotropic medium has traditionally been a standard assumption in the field of modeling and design of borehole heat exchangers for shallow geothermal applications, although such ideal conditions are rare in actual subsurface environments. With the growing interest in large-scale HT-BTES systems, adequate practises for characterizing and accounting for the geological and hydrogeological conditions at the storage site are required for successful design and performance evaluation of the system, as well as for assessing the impact of the BTES on the surrounding environment.

Because of the compositional and spatial diversity of hydrogeological conditions found at different scales and sites, there is no universally valid approach for characterizing and modeling subsurface flow and transport processes. Recent and ongoing research on coupled subsurface hydro-thermal processes in porous and fractured media has provided a robust and comprehensive framework for modeling complex flow and transport processes in a wide variety of hydrogeological settings to face this challange. These modeling concepts, typically based on deterministic and stochastic continuum or DFN approaches, have now become become well-established in hydrogeologic practice. Future exploration of their applicability also in the context of BTES modeling could provide a basis for more accurate prediction of the subsurface temperatures within the storage.

It follows from the site-specific nature of any groundwater flow and transport problem that general guidelines on groundwater effects on BTES design and performance are difficult to provide. Instead, an individual assessment is typically required for each case, and a numerical approach to the study of actual coupled flow and transport problems is usually needed. In this work, a FEM pure heat conduction model has been applied to simulate the operation of an existing HT-BTES located in dry heterogeneous soil. To replicate the actual BTES operation, a FEFLOW plugin tool for enabling control of flow direction through series-connected BHEs has been developed and validated against operational and monitoring data. The plugin tool was shown to be capable of accurately predicting the long-term thermal dynamics of the BHEs and the storage medium. However, further evaluation is required for assessing its applicability for shorter-term problems.

The validated pure conduction model provided a benchmark by which to compare the behaviour of the BTES under influence of groundwater flow. Numerical experiments were conducted by assuming a hypothetical groundwater flow system within the model domain. The simulations demonstrate that the thermal behaviour of a BTES in a conduction-dominated environment is fundamentally different from that in an advection-dominated environment. In the pre-investigation and design process for HT-BTES systems, appropriate and sufficient information should therefore be collected to assess the validity and applicability of assuming either conduction or combined conduction-advection heat transport in the ground.

Based on KPIs in terms of energy and exergy efficiencies evaluated at a system as well as a storage level, a performance evaluation study has been carried out to quantify how the occurrence of groundwater flow affect the amount and quality of the heat being stored and exchanged. Adding exergy next to conventional performance figures based on energy efficiency may contribute to a more comprehensive understanding of the thermal behaviour and performance of the BTES system as it can reflect the energy usability under different operation conditions and allow for identifying sources of inefficiencies throughout the storing cycles. Based on the performance evaluation study, it was shown that high groundwater flow rates are in general detrimental to the performance in terms of seasonal system energy and exergy efficiency, as well storage energy efficiency. The results indicate, however, that small groundwater flow rates can have a slight positive effect on the system level performance due to enhanced heat transport driven by advection. Advective effects on storage exergy performance were found to be less pronounced, which could be an effect of other major mechanisms contributing to temperature degradation under investigated conditions.

Future studies are called for to further evaluate HT-BTES performance under a wider range of time scales, BHE designs, operation conditions and subsurface conditions. A numerical approach as is used in this work can be applied for simulations with a high level of detail and accuracy, although this comes with a high

computational burden. Therefore, it is recommended to explore the use of analytical methods for conducting extensive parametric studies.

Bibliography

Adler, P.M., 1999. Fractures and Fracture Networks, Theory and Applications of Transport in Porous Media, 15. Springer Netherlands, Dordrecht.

Al-Khoury, R., Bonnier, P.G., 2006. Efficient finite element formulation for geothermal heating systems. Part II: transient. International Journal for Numerical Methods in Engineering 67, 725–745. https://doi.org/10.1002/nme.1662

Al-Khoury, R., Bonnier, P.G., Brinkgreve, R.B.J., 2005. Efficient finite element formulation for geothermal heating systems. Part I: steady state. International Journal for Numerical Methods in Engineering 63, 988–1013. https://doi.org/10.1002/nme.1313

Andújar Márquez, J.M., Martínez Bohórquez, M.Á., Gómez Melgar, S., 2016. Ground Thermal Diffusivity Calculation by Direct Soil Temperature Measurement. Application to very Low Enthalpy Geothermal Energy Systems. Sensors (Basel) 16. https://doi.org/10.3390/s16030306

Angelotti, A., Alberti, L., La Licata, I., Antelmi, M., 2014. Energy performance and thermal impact of a Borehole Heat Exchanger in a sandy aquifer: Influence of the groundwater velocity. Energy Conversion and Management 77, 700–708. https://doi.org/10.1016/j.enconman.2013.10.018

ASHRAE, 2015. 34. Geothermal Energy, in: 2015 ASHRAE Handbook - Heating, Ventilating, and Air-Conditioning Applications. American Society of Heating Refrigerating and Air-Conditioning Engineers, Inc.

Banks, D., 2015. A review of the importance of regional groundwater advection for ground heat exchange. Environ Earth Sci 73, 2555–2565. https://doi.org/10.1007/s12665-014-3377-4

Bauer D., Heidemann W., Müller-Steinhagen H., Diersch H.-J. G., 2011. Thermal resistance and capacity models for borehole heat exchangers. International Journal of Energy Research 35, 312–320. https://doi.org/10.1002/er.1689

Bauer, D., Heidemann, W., Müller-Steinhagen, H., G Diersch, H.-J., 2009. MODELLING AND SIMULATION OF GROUNDWATER INFLUENCE ON BOREHOLE THERMAL ENERGY STORES, in: Proceedings of Effstock, the 11th International Conference on Thermal Energy Storage. Stockholm, Sweden.

Bear, J., 1972. Dynamics of Fluids in Porous Media. Dover Publications, New York.

Bear, J., Tsang, C.F., de Marsily, G., 1993. Flow and contaminant transport in fractured rocks. Academic Press, San Diego, CA United States.

Bear, J.J., Cheng, H.-D.A., 2010. Modeling Groundwater Flow and Contaminant Transport, Theory and Applications of Transport in Porous Media. Springer, Dordrecht. https://doi.org/10.1007/978-1-4020-6682-5_1

Berkowitz, B., 2002. Characterizing flow and transport in fractured geological media: A review. Advances in Water Resources 25, 861–884. https://doi.org/10.1016/S0309-1708(02)00042-8

Bernier, M.A., 2001. Ground-coupled heat pump system simulation. ASHRAE Transactions 107, 605–616.

Berre, I., Doster, F., Keilegavlen, E., 2018. Flow in Fractured Porous Media: A Review of Conceptual Models and Discretization Approaches. Transp Porous Med. https://doi.org/10.1007/s11242-018-1171-6

Bianchi, G., Panayiotou, G.P., Aresti, L., Kalogirou, S.A., Florides, G.A., Tsamos, K., Tassou, S.A., Christodoulides, P., 2019. Estimating the waste heat recovery in the European Union Industry. Energ. Ecol. Environ. 4, 211–221. https://doi.org/10.1007/s40974-019-00132-7

BLOCON, 2017. EED version 4.

Carslaw, H.S., Jaeger, J.C., 1959. Conduction of Heat In Solids. Oxford science publications, Oxford.

Catolico, N., Ge, S., McCartney, J.S., 2016. Numerical Modeling of a Soil-Borehole Thermal Energy Storage System 15. https://doi.org/10.2136/vzj2015.05.0078

Chapuis, S., Bernier, M., 2009. Seasonal Storage of Solar Energy in Borehole Heat Exchangers. Presented at the Eleventh International IBPSA Conference, Glasgow, Scotland, pp. 599–606.

Chen, R., 2010. Groundwater inflow into rock tunnels (thesis).

Chen, T., Clauser, C., Marquart, G., 2017. Efficiency and accuracy of equivalent fracture models for predicting fractured geothermal reservoirs: the influence of fracture network patterns. Energy Procedia 125, 318–326. https://doi.org/10.1016/j.egypro.2017.08.206

Chiasson, A., O'Connell, A., 2011. New analytical solution for sizing vertical borehole ground heat exchangers in environments with significant groundwater flow: Parameter estimation from thermal response test data. HVAC&R Research 17, 1000–1011. https://doi.org/10.1080/10789669.2011.609926

Chiasson, A.C., Rees, S.J., Spitler, J.D., 2000. A Preliminary Assessment Of The Effects Of Ground-Water Flow On Closed-Loop Ground-Source Heat Pump Systems. ASHRAE Transactions 106, 380–393.
Choi, J.C., Park, J., Lee, S.R., 2013. Numerical evaluation of the effects of groundwater flow on borehole heat exchanger arrays. Renewable Energy 52, 230–240. https://doi.org/10.1016/j.renene.2012.10.028
Cimmino, M., Bernier, M., Adams, F., 2013. A contribution towards the determination of g-functions using the finite line source. Applied Thermal Engineering 51, 401–412. https://doi.org/10.1016/j.applthermaleng.2012.07.044
Dehkordi, S.E., Olofsson, B., Schincariol, R.A., 2015a. Effect of groundwater flow in vertical and horizontal fractures on borehole heat exchanger temperatures. Bull Eng Geol Environ 74, 479–491. https://doi.org/10.1007/s10064-014-0626-4
Dehkordi, S. Emad, Schincariol, R.A., 2014. Effect of thermal-hydrogeological and borehole heat exchanger properties on performance and impact of vertical closed-loop geothermal heat pump systems. Hydrogeol J 22, 189–203. https://doi.org/10.1007/s10040-013-1060-6
Dehkordi, S.E., Schincariol, R.A., 2014. Guidelines and the design approach for vertical geothermal heat pump systems: current status and perspective. Can. Geotech. J. 51, 647–662. https://doi.org/10.1139/cgj-2012-0205
Dehkordi, S.E., Schincariol, R.A., Olofsson, B., 2015b. Impact of Groundwater Flow and Energy Load on Multiple Borehole Heat Exchangers. Groundwater 53, 558–571. https://doi.org/10.1111/gwat.12256
DHI-WASY, 2010. FEFLOW White Papers Vol. 5.
DHI-WASY, 2009. FEFLOW White Papers Vol. I.
Diao, N., Li, Q., Fang, Z., 2004. Heat transfer in ground heat exchangers with groundwater advection. International Journal of Thermal Sciences 43, 1203–1211. https://doi.org/10.1016/j.ijthermalsci.2004.04.009
Diersch, H.-J.G., 2014. FEFLOW Finite Element Modeling of Flow, Mass and Heat Transport in Porous and Fractured Media. Springer Berlin Heidelberg, Berlin, Heidelberg.
Diersch, H.-J.G., Bauer, D., 2014. Analysis, modeling and simulation of underground thermal energy storage (UTES) systems. Elsevier Inc.
Diersch, H.-J.G., Bauer, D., Heidemann, W., Rühaak, W., Schätzl, P., 2011a. Finite element modeling of borehole heat exchanger systems: Part 2. Numerical simulation. Computers & Geosciences 37, 1136–1147. https://doi.org/10.1016/j.cageo.2010.08.002
Diersch, H.-J.G., Bauer, D., Heidemann, W., Rühaak, W., Schätzl, P., 2011b. Finite element modeling of borehole heat exchanger systems: Part 1. Fundamentals. Computers & Geosciences 37, 1122–1135. https://doi.org/10.1016/j.cageo.2010.08.003
Dietrich, P., Helmig, R., Sauter, M., Hötzl, H., Köngeter, J., Teutsch, G. (Eds.), 2005. Flow and Transport in Fractured Porous Media. Springer-Verlag, Berlin/Heidelberg. https://doi.org/10.1007/b138453
Dincer, I., Rosen, M.A., 2007. Chapter 9 - EXERGY ANALYSIS OF THERMAL ENERGY STORAGE SYSTEMS, in: Dincer, I., Rosen, M.A. (Eds.), EXERGY. Elsevier, Amsterdam, pp. 127–162. https://doi.org/10.1016/B978-008044529-8.50012-4
Eskilson, P., 1987. Thermal analysis of heat extraction boreholes. Department of Mathematical Physics, University of Lund, Lund, Sweden.
Eskilson, P., Claesson, J., 1988. Simulation Model for Thermally Interacting Heat Extraction Boreholes. Numerical Heat Transfer 13, 149–165. https://doi.org/10.1080/10407788808913609
Gehlin, S.E.A., Hellström, G., 2003. Influence on thermal response test by groundwater flow in vertical fractures in hard rock. Renewable Energy 28, 2221–2238. https://doi.org/10.1016/S0960-1481(03)00128-9
GEUS [WWW Document], n.d. URL http://www.geus.dk/ (accessed 12.4.20).
Grycz, D., Hemza, P., Rozehnal, Z., 2014. Charging of the Experimental High Temperature BTES Via CHP Unit - Early Results. Energy Procedia, Proceedings of the 2nd International Conference on Solar Heating and Cooling for Buildings and Industry (SHC 2013) 48, 355–360. https://doi.org/10.1016/j.egypro.2014.02.041
Heath, R.C., 1983. Basic ground-water hydrology. USGeological Survey ;--For sale by Distribution Branch, Text Products Section, USGeological Survey,.
Hellström, G., 1991. Ground heat storage : thermal analyses of duct storage systems.
Hepbasli, A., 2005. Thermodynamic analysis of a ground-source heat pump system for district heating. International Journal of Energy Research 29, 671–687. https://doi.org/10.1002/er.1099

Hu, J., 2017. An improved analytical model for vertical borehole ground heat exchanger with multiple-layer substrates and groundwater flow. Applied Energy 202, 537–549. https://doi.org/10.1016/j.apenergy.2017.05.152

Ingersoll, L.R., Zobel, O.J., Ingersoll, A.C., 1954. Heat Conduction With Engineering, Geological, and Other Applications, Revised edition. ed. University of Wisconsin Press.

Jacquey, A.B., 2017. Coupled Thermo-Hydro-Mechanical Processes in Geothermal Reservoirs:

Joyce, S., Hartley, L., Applegate, D., Hoek, J., Jackson, P., 2014. Multi-scale groundwater flow modeling during temperate climate conditions for the safety assessment of the proposed high-level nuclear waste repository site at Forsmark, Sweden. Hydrogeol J 22, 1233–1249. https://doi.org/10.1007/s10040-014-1165-6

Kalinina, E., McKenna, S.A., Klise, K.A., Hadgu, T., Lowry, T.S., 2012. Incorporating Complex Three-Dimensional Fracture Networks Into Geothermal Reservoir Simulation. GRC Transactions 36, 6.

Karimzade, E., Sharifzadeh, M., Zarei, H.R., Shahriar, K., Cheraghi Seifabad, M., 2017. Prediction of water inflow into underground excavations in fractured rocks using a 3D discrete fracture network (DFN) model. Arab J Geosci 10, 206. https://doi.org/10.1007/s12517-017-2987-z

Katsura, T., Shoji, Y., Sakata, Y., Nagano, K., 2020. Method for calculation of ground temperature in scenario involving multiple ground heat exchangers considering groundwater advection. Energy and Buildings 220, 110000. https://doi.org/10.1016/j.enbuild.2020.110000

Kizilkan, O., Dincer, I., 2012. Exergy analysis of borehole thermal energy storage system for building cooling applications. Energy and Buildings 49, 568–574. https://doi.org/10.1016/j.enbuild.2012.03.013

Klepikova, M., 2013. Imaging of fractured rock properties from flow and heat transport : field experiments and inverse modelling (phdthesis). Université Rennes 1.

Konikow, L.F., 2011. The Secret to Successful Solute-Transport Modeling. Groundwater 49, 144–159. https://doi.org/10.1111/j.1745-6584.2010.00764.x

Lakshmanan, E., 2011. Hydraulic Conductivity - Issues, Determination and Applications.

Lamarche, L., Beauchamp, B., 2007. A new contribution to the finite line-source model for geothermal boreholes. Energy and Buildings 39, 188–198. https://doi.org/10.1016/j.enbuild.2006.06.003

Lanini, S., Delaleux, F., Py, X., R.Olivès, Nguyen, D., 2014. Improvement of borehole thermal energy storage design based on experimental and modelling results. Energy and Buildings 77, 393–400. https://doi.org/10.1016/j.enbuild.2014.03.056

Lazzarotto, A., Mazzotti Pallard, W., Abuasbeh, M., Acuña, J., 2020. Performance Evaluation of Borehole Thermal Energy Storage Systems Through Energy and Exergy Analysis. Presented at the World Geothermal Congress 2020, Reykjavik.

Le Borgne, T.L., Bour, O., Dreuzy, J.R. de, Davy, P., Touchard, F., 2004. Equivalent mean flow models for fractured aquifers: Insights from a pumping tests scaling interpretation. Water Resources Research 40. https://doi.org/10.1029/2003WR002436

Luo, J., Rohn, J., Bayer, M., Priess, A., Xiang, W., 2014. Analysis on performance of borehole heat exchanger in a layered subsurface. Applied Energy 123, 55–65. https://doi.org/10.1016/j.apenergy.2014.02.044

Luo, J., Rohn, J., Xiang, W., Bertermann, D., Blum, P., 2016. A review of ground investigations for ground source heat pump (GSHP) systems. Energy and Buildings 117, 160–175. https://doi.org/10.1016/j.enbuild.2016.02.038

Maréchal, J.C., Dewandel, B., Subrahmanyam, K., 2004. Use of hydraulic tests at different scales to characterize fracture network properties in the weathered-fractured layer of a hard rock aquifer. Water Resources Research 40. https://doi.org/10.1029/2004WR003137

Mielke, P., Bauer, D., Homuth, S., Götz, A.E., Sass, I., 2014. Thermal effect of a borehole thermal energy store on the subsurface. Geothermal Energy 2, 5. https://doi.org/10.1186/s40517-014-0005-1

Molina-Giraldo, N., Bayer, P., Blum, P., 2011a. Evaluating the influence of thermal dispersion on temperature plumes from geothermal systems using analytical solutions. International Journal of Thermal Sciences 50, 1223–1231. https://doi.org/10.1016/j.ijthermalsci.2011.02.004

Molina-Giraldo, N., Blum, P., Zhu, K., Bayer, P., Fang, Z., 2011b. A moving finite line source model to simulate borehole heat exchangers with groundwater advection. International Journal of Thermal Sciences 50, 2506–2513. https://doi.org/10.1016/j.ijthermalsci.2011.06.012

Moradi, A., Smits, K.M., Massey, J., Cihan, A., McCartney, J., 2015. Impact of coupled heat transfer and water flow on soil borehole thermal energy storage (SBTES) systems: Experimental and modeling investigation. Geothermics 57, 56–72. https://doi.org/10.1016/j.geothermics.2015.05.007

Nastev, M., Savard, M.M., Lapcevic, P., Lefebvre, R., Martel, R., 2004. Hydraulic properties and scale effects investigation in regional rock aquifers, south-western Quebec, Canada. Hydrogeology Journal 12, 257–269. https://doi.org/10.1007/s10040-004-0340-6

Neuman, S.P., 2005. Trends, prospects and challenges in quantifying flow and transport through fractured rocks. Hydrogeol J 13, 124–147. https://doi.org/10.1007/s10040-004-0397-2

Neuman, S.P., 1990. Universal scaling of hydraulic conductivities and dispersivities in geologic media. Water Resources Research 26, 1749–1758. https://doi.org/10.1029/WR026i008p01749

Nguyen, A., Pasquier, P., Marcotte, D., 2017. Borehole thermal energy storage systems under the influence of groundwater flow and time-varying surface temperature. Geothermics 66, 110–118. https://doi.org/10.1016/j.geothermics.2016.11.002

Nguyen, A., Pasquier, P., Marcotte, D., 2015. Influence of groundwater flow in fractured aquifers on standing column wells performance. Geothermics 58, 39–48. https://doi.org/10.1016/j.geothermics.2015.08.005

Nilsson, E., 2020. Borehole Thermal Energy Storage Systems for Storage of Industrial Excess Heat : Performance Evaluation and Modelling.

Nordell, B., 1994. Borehole Heat Store Design Optimization. Luleå University of Technology, Luleå.

Nordell, B., Scorpo, A.L., Andersson, O., Rydell, L., Carlsson, B., 2016. Long-term Long Term Evaluation of Operation and Design of the Emmaboda BTES. : Operation and Experiences 2010-2015. Luleå tekniska universitet.

Nußbicker, J., Mangold, D., Heidemann, W., Müller-Steinhagen, H., 2003. Solar Assisted District Heating System with Duct Heat Store in Neckarsulm-Amorbach (Germany).

Ozgener, L., Hepbasli, A., Dincer, I., 2005. Energy and exergy analysis of geothermal district heating systems: an application. Building and Environment 40, 1309–1322. https://doi.org/10.1016/j.buildenv.2004.11.001

Ozudogru, T.Y., Ghasemi-Fare, O., Olgun, C.G., Basu, P., 2015. Numerical Modeling of Vertical Geothermal Heat Exchangers Using Finite Difference and Finite Element Techniques. Geotech Geol Eng 33, 291–306. https://doi.org/10.1007/s10706-014-9822-z

Pacheco, F.A.L., 2013. Hydraulic diffusivity and macrodispersivity calculations embedded in a geographic information system. Hydrological Sciences Journal 58, 930–944. https://doi.org/10.1080/02626667.2013.784847

Pahud, D., Hellström, G., Mazzarella, L., 1996. Heat Storage in the Ground. Duct Ground Heat Storage Model for TRNSYS (TRNVDST). User Manual for the October 1996 Version (Report). Ecole Polytechnique Fédérale de Lausanne.

Pruess, K., 1985. A Practical Method for Modeling Fluid and Heat Flow in Fractured Porous Media. Society of Petroleum Engineers Journal 25, 14–26. https://doi.org/10.2118/10509-PA

Rapantova, N., Pospisil, P., Koziorek, J., Vojcinak, P., Grycz, D., Rozehnal, Z., 2016. Optimisation of experimental operation of borehole thermal energy storage. Applied Energy 181, 464–476. https://doi.org/10.1016/j.apenergy.2016.08.091

Rezaie, B., Reddy, B.V., Rosen, M.A., 2015. Exergy analysis of thermal energy storage in a district energy application. Renewable Energy 74, 848–854. https://doi.org/10.1016/j.renene.2014.09.014

Rivera, J.A., Blum, P., Bayer, P., 2015. Analytical simulation of groundwater flow and land surface effects on thermal plumes of borehole heat exchangers. Applied Energy 146, 421–433. https://doi.org/10.1016/j.apenergy.2015.02.035

Rovey, C.W., 1994. Assessing flow systems in carbonate aquifers using scale effects in hydraulic conductivity. Geo 24, 244–253. https://doi.org/10.1007/BF00767085

Rybach, L., Eugster, W.J., 2010. Sustainability aspects of geothermal heat pump operation, with experience from Switzerland. Geothermics, Special Issue on the Sustainable Utilization of Geothermal Energy 39, 365–369. https://doi.org/10.1016/j.geothermics.2010.08.002

Rybach, L., Mongillo, M., 2006. Geothermal sustainability-A review with identified research needs. Transactions - Geothermal Resources Council 30, 1083–1090.

Selroos, J.-O., Walker, D.D., Ström, A., Gylling, B., Follin, S., 2002. Comparison of alternative modelling approaches for groundwater flow in fractured rock. Journal of Hydrology 257, 174–188. https://doi.org/10.1016/S0022-1694(01)00551-0

Shapiro, A.M., 1987. Transport Equations for Fractured Porous Media, in: Bear, J., Corapcioglu, M.Y. (Eds.), Advances in Transport Phenomena in Porous Media, NATO ASI Series. Springer Netherlands, Dordrecht, pp. 405–471. https://doi.org/10.1007/978-94-009-3625-6_10

Sharqawy, M.H., Mokheimer, E.M., Habib, M.A., Badr, H.M., Said, S.A., Al-Shayea, N.A., 2009. Energy, exergy and uncertainty analyses of the thermal response test for a ground heat exchanger. International Journal of Energy Research 33, 582–592. https://doi.org/10.1002/er.1496

Shewchuk, J.R., 1996. Triangle: Engineering a 2D quality mesh generator and Delaunay triangulator, in: Lin, M.C., Manocha, D. (Eds.), Applied Computational Geometry Towards Geometric Engineering, Lecture Notes in Computer Science. Springer, Berlin, Heidelberg, pp. 203–222. https://doi.org/10.1007/BFb0014497

Signorelli, S., Kohl, Tomas, Rybach. Ladislaus, 2005. SUSTAINABILITY OF PRODUCTION FROM BOREHOLE HEAT EXCHANGER FIELDS, in: Proceedings of World Geothermal Congress 2005. Antalaya.

Sommer, W., Valstar, J., Gaans, P. van, Grotenhuis, T., Rijnaarts, H., 2013. The impact of aquifer heterogeneity on the performance of aquifer thermal energy storage. Water Resources Research 49, 8128–8138. https://doi.org/10.1002/2013WR013677

Sørensen, P.A., Larsen, J., Thøgersen, L., Andersen, J.D., Østergaard, C., Schmidt, T., 2013. Boreholes in Brædstrup. Final report.

Spitler, J.D., Bernier, M., 2016. 2 - Vertical borehole ground heat exchanger design methods, in: Rees, S.J. (Ed.), Advances in Ground-Source Heat Pump Systems. Woodhead Publishing, pp. 29–61. https://doi.org/10.1016/B978-0-08-100311-4.00002-9

Sutton, M.G., Nutter, D.W., Couvillion, R.J., 2003. A Ground Resistance for Vertical Bore Heat Exchangers With Groundwater Flow. J. Energy Resour. Technol 125, 183–189. https://doi.org/10.1115/1.1591203

Tordrup, K. W., Poulsen, S.E., Bjørn, H., 2017. An improved method for upscaling borehole thermal energy storage using inverse finite element modelling. Renewable Energy 105, 13–21. https://doi.org/10.1016/j.renene.2016.12.011

Tordrup, K.W., Poulsen, S.E., Bjørn, H., 2016. Calibration of a finite element model of a borehole thermal energy storage in FEFLOW: model and numerical considerations. Presented at the European Geothermal Congress, Strasbourg, p. 6.

Tordrup, Karl Woldum, Poulsen, U.V., Nielsen, C., 2017. A modular approach to inverse modelling of a district heating facility with seasonal thermal energy storage. Energy Procedia, 11th International Renewable Energy Storage Conference, IRES 2017, 14-16 March 2017, Düsseldorf, Germany 135, 263–271. https://doi.org/10.1016/j.egypro.2017.09.518

Tsang, C.-F., 1990. The Modeling Process and Model Validation. Ground Water 29.

U.S. National Committee for Rock Mechanics, 1996. Rock fractures and fluid flow contemporary understanding and applications. National Academy Press, Washington, D.C.

Wheatcraft, S.W., Tyler, S.W., 1988. An explanation of scale-dependent dispersivity in heterogeneous aquifers using concepts of fractal geometry. Water Resources Research 24, 566–578. https://doi.org/10.1029/WR024i004p00566

Wheatcroft, E., Wynn, H., Lygnerud, K., Bonvicini, G., Leonte, D., 2020. The Role of Low Temperature Waste Heat Recovery in Achieving 2050 Goals: A Policy Positioning Paper. Energies 13, 2107. https://doi.org/10.3390/en13082107

Yang, W., Chen, Y., Shi, M., Spitler, J.D., 2013. Numerical investigation on the underground thermal imbalance of ground-coupled heat pump operated in cooling-dominated district. Applied Thermal Engineering 58, 626–637. https://doi.org/10.1016/j.applthermaleng.2013.04.061

Zeng, H.Y., Diao, N.R., Fang, Z.H., 2002. A finite line-source model for boreholes in geothermal heat exchangers. Heat Trans. Asian Res. 31, 558–567. https://doi.org/10.1002/htj.10057

Zhang, C., Wang, Y., Liu, Y., Kong, X., Wang, Q., 2018. Computational methods for ground thermal response of multiple borehole heat exchangers: A review. Renewable Energy 127, 461–473. https://doi.org/10.1016/j.renene.2018.04.083

Zhang, L., Zhao, L., Yang, L., Hu Songtao, 2015. Analyses on soil temperature responses to intermittent heat rejection from BHEs in soils with groundwater advection. Energy and Buildings 107, 355–365. https://doi.org/10.1016/j.enbuild.2015.08.040